Cell Reports

Supplemental Information

YAP Inhibition Restores Hepatocyte Differentiation in Advanced HCC leading to Tumor Regression

Julien Fitamant, Filippos Kottakis, Samira Benhamouche, Helen S. Tian, Nicolas Chuvin, Christine A. Parachoniak, Julia M. Nagle, Rushika M. Perera, Marjorie Lapouge, Vikram Deshpande, Andrew X. Zhu, Albert Lai, Bosun Min, Yujin Hoshida, Joseph Avruch, Daniela Sia, Genís Campreciós, Andrea I. McClatchey, Josep M. Llovet, David Morrissey, Lakshmi Raj, and Nabeel Bardeesy

Figure S1 (related to Figure 1)

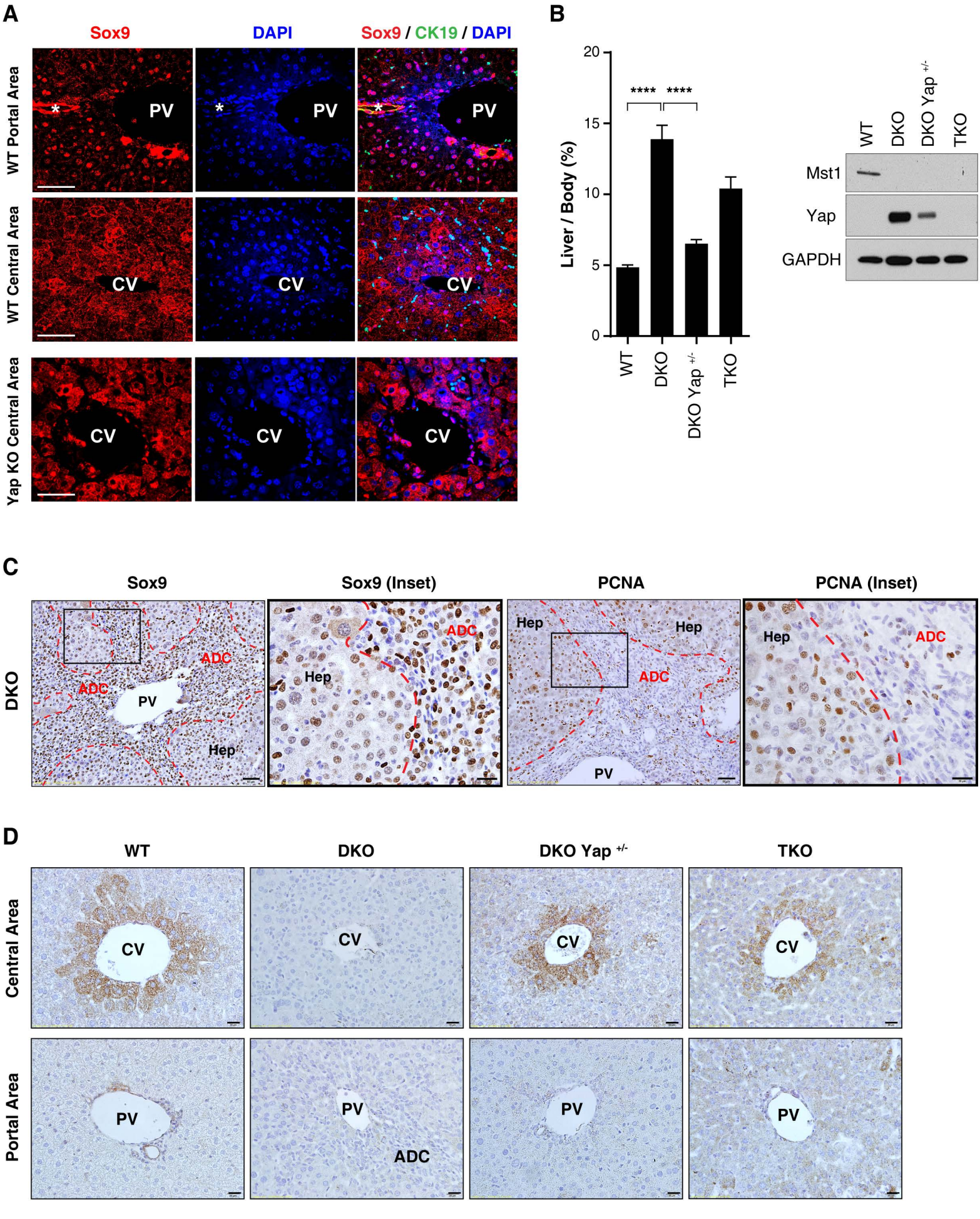

Figure S1. The Hippo pathway controls hepatocyte identity (related to Figure 1).

(A) SOX9 immunofluorescence in livers from WT and *Yap* KO mice. CK19 is a biliary marker. Bile ducts are indicated by an asterisk. Scale bar, 50μm.

(B) *Left panel:* Quantification of liver mass to body mass in mice of the indicated genotypes. N= 7 mice per group. Error bars indicate S.E.M. ****p<0.0001. *Right panel*: Immunoblot analysis of Mst1 and Yap in whole liver extracts of the indicated genotypes.

(C) PCNA and SOX9 staining in livers from DKO mice in regions with hepatocyte (Hep) and atypical ductal cell (ADC) morphology. Note that a higher proportion of the hepatocyte-like cells stain positively for PCNA as compared to the ADCs. Scale bars: 50 μm and 20 μm (Inset).

(D) Immunohistochemical analysis for the pericentral marker ornithine aminotransferase (OAT) in 7-week old livers of the indicated genotypes. Scale bar: 20μm.

PV: Portal vein, CV: Central vein, ADC: Atypical ductal cells.

Figure S2 (related to Figure 2)

A

TEAD/TEF1 enrichment binding sites

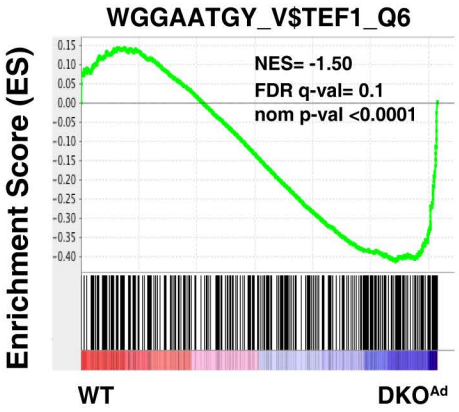

B

Prediction of Yap-regulated transcriptional circuitry (normal liver)

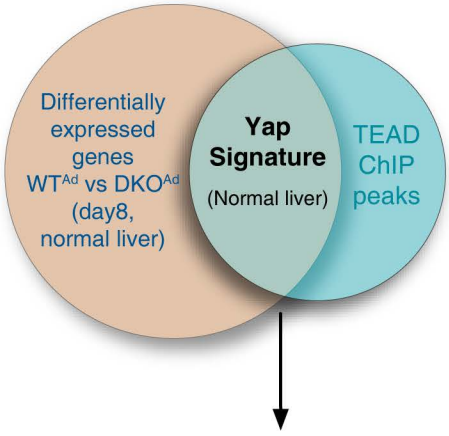

Identification of enriched transcription factors
(among 281 anayzed) using ENCODE ChIP-seq data

Factor	*Total genes bound by factor*	*YAP/TEAD targets bound (out of 912)*	*Q-value (Hypergeometric test: Benjamini-Hochberg)*	*Factor rank*
P300	11814	726	1.975E-42	1
Foxa1	**8765**	**574**	**5.162E-33**	**2**
Hnf4g	**3740**	**320**	**5.162E-33**	**3**
Hdac2	7939	535	8.517E-33	4
Tbp	12799	740	1.196E-32	5
Nfic	6462	462	2.701E-32	6
Mxi1	11719	696	5.151E-32	7
Hnf4a	**3876**	**324**	**6.113E-32**	**8**
Taf1	13370	759	6.528E-32	9
Cebpd	**5434**	**408**	**7.106E-32**	**10**

Figure S2. Identification of candidate direct YAP targets following acute *Mst1/Mst2* inactivation in the adult liver (related to Figure 2).

(A) GSEA of differentially expressed genes in DKO^{Ad} versus WT^{Ad} livers (8 days after Adeno-Cre administration) showing a significant enrichment of the consensus TEAD/TEF-1 DNA binding motif in the promoter sequences of this gene set.

(B) *Top panel:* To predict transcriptional networks regulated by YAP, we first identified presumptive direct YAP target genes (YAP signature) by integrating the set of differentially expressed genes observed in DKO^{Ad} versus WT^{Ad} livers (day 8) with ChIP-seq data for TEAD binding sites in hepatic cells (HepG2 cells) from the ENCODE database: http://encodeqt.simple-encode.org/). We then determined the enrichment of additional transcription factor binding sites in the region from -5 kb to +2.5 kb relative to the transcriptional start sites of this gene set using the data from ENCODE (comprising ChIP-seq data for 281 transcription factors). *Bottom panel:* The chart shows strong enrichment for FOXA1 and HNF4A binding to this set of candidate YAP targets, suggesting interplay of YAP and these transcription factors in regulating hepatocyte quiescence and differentiation. The top ranked transcription factors by enrichment score are shown. General transcription factors are greyed-out.

Figure S3 (related to Figure 3)

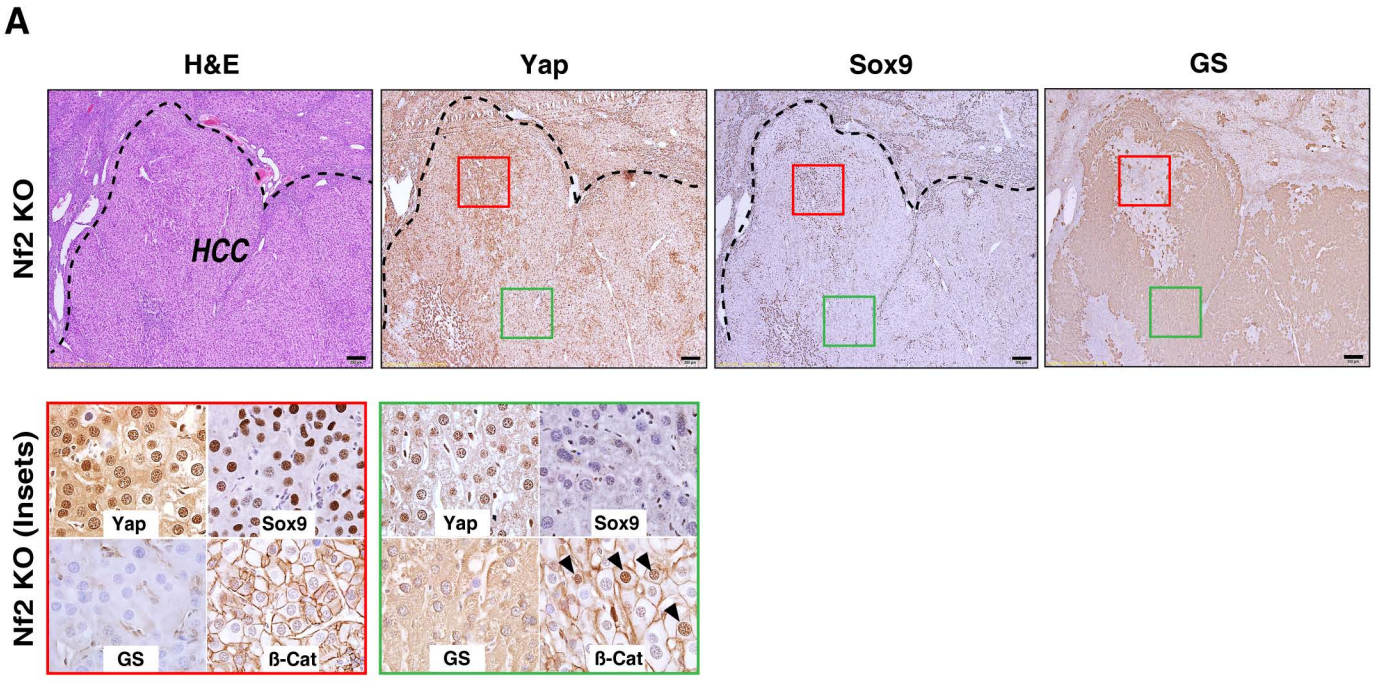

Figure S3. Analysis of *Nf2* KO HCCs (related to Figure 3).

(A) HCCs in mice with liver-specific *Nf2* KO show tumor variable levels of YAP staining, with high YAP specifically correlating with nuclear SOX9 and absence of GS and nuclear β-catenin. Arrowheads indicate nuclear β-catenin. The insets show high magnification views and are color-coded with the corresponding boxed regions. Scale bar: 200 μm.

Figure S4 (related to Figure 4)

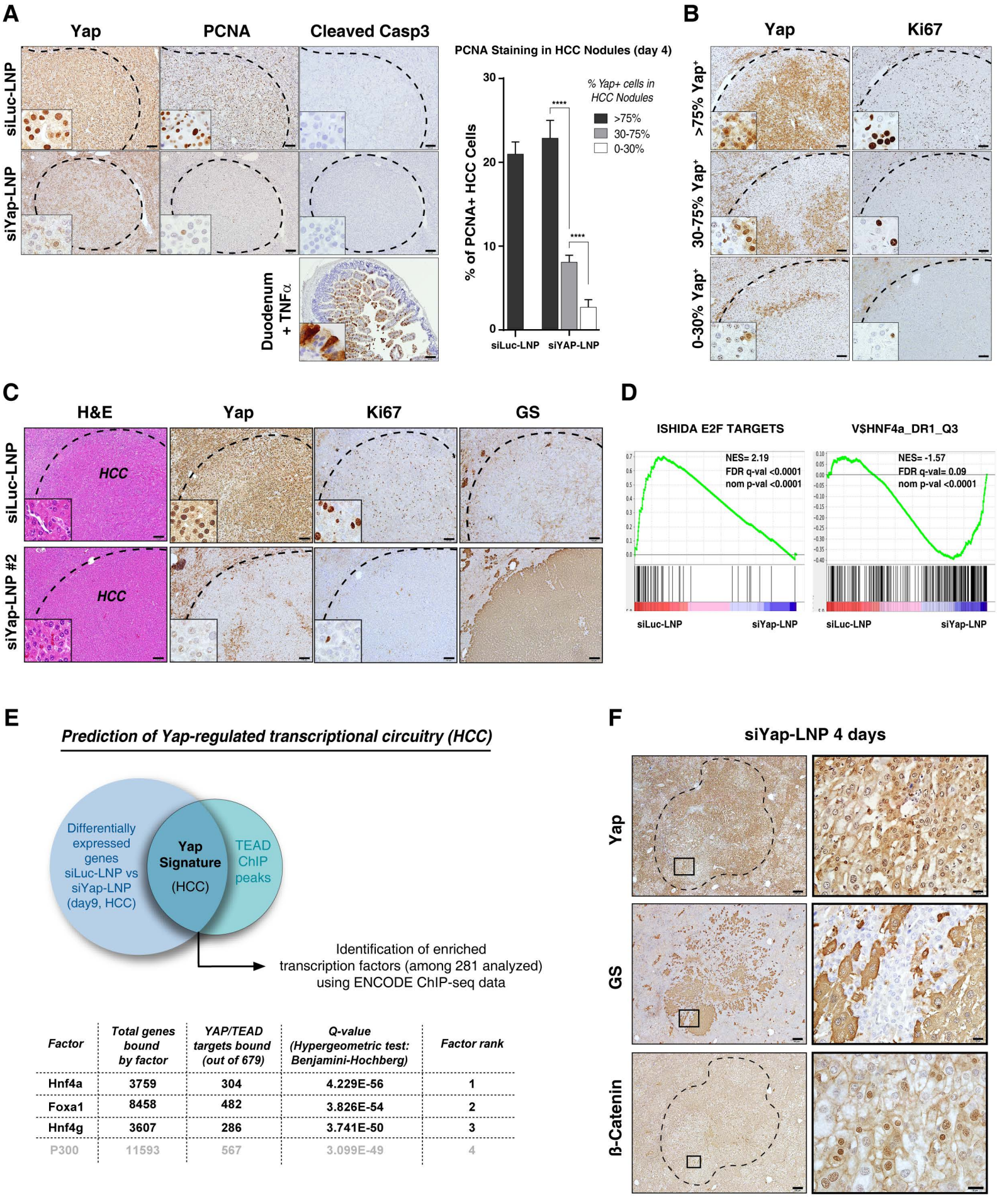

Factor	Total genes bound by factor	YAP/TEAD targets bound (out of 679)	Q-value (Hypergeometric test: Benjamini-Hochberg)	Factor rank
Hnf4a	3759	304	4.229E-56	1
Foxa1	8458	482	3.826E-54	2
Hnf4g	3607	286	3.741E-50	3
P300	11593	567	3.099E-49	4

Figure S4. siYap-LNPs induce proliferative arrest and reactivate a hepatocyte differentiation program in advanced HCC (related to Figure 4).

(A) Representative immunohistochemical staining for YAP, PCNA and cleaved caspase-3 (Casp3) in HCCs following 4 days treatment with the indicated siRNA-LNP formulations. The bottom panel shows a positive control for cleaved caspase-3 staining (duodenal tissue from mouse treated with TNFα). The PCNA staining data are quantified in the graph (*right* panel). The chart shows % PCNA-positive HCC cells in different tumor nodules grouped according to degree of *Yap* knockdown. Note that the decrease in PCNA staining correlates with effectiveness of Yap knockdown. N= 87 tumors (siLuc; from treated 5 mice) and 87 tumors (siYap; from 4 treated mice). Error bars indicate S.E.M. ****p<0.0001. Scale bar: 100 μm.

(B) Immunohistochemical staining for YAP and Ki67 in HCCs following 9 days treatment with siYap-LNP formulation showing representative nodules with varying degrees of *Yap* knockdown. Note that the decreased proliferation of HCC cells is directly correlated with the proportion of *Yap* knockdown. The percentage of YAP-positive HCC cells following treatment is indicated on the left side.

(C) Representative immunohistochemical staining for YAP, Ki67 and GS in HCCs following 9 days treatment with a second siYap-LNP formulation (siYap-LNP#2). Scale bar: 100 μm.

(D) GSEA of differentially expressed genes in siLuc-LNPs versus siYap-LNPs-treated HCCs following 9 days of treatment. *Yap* knockdown results in downregulation of proliferation/E2F target gene signature and by reactivation of known Hnf4α target genes.

(E) *Top panel*: A YAP-specific activation signature in HCC was established by integrating the set of differentially expressed genes observed in siLuc-LNP-treated vs siYap-LNP-treated HCCs at day 9 with ChIP-seq data for TEAD binding sites in hepatic cells (ENCODE database). This allowed the identification of differentially expressed genes with predicted TEAD binding sites in their promoters to be analyzed for other enriched binding sites (-5 kb to +2.5 kb from the

transcriptional start sites). *Bottom panel*: the chart shows most enriched transcription factors (from Encode database, which includes ChIP-seq profiles for 281 transcription factors). Key regulators of liver differentiation are highlighted. General transcription factors are greyed-out.

(F) Representative immunohistochemical staining for YAP, GS and β-catenin showing that siYap-LNPs induce partial reactivation of a WNT/β–catenin program in a subset of HCC nodules after only 3 days of treatment. Areas of β-catenin reactivation correlate with regions displaying low YAP staining. Scale bars: 200 μm and 20 μm (Inset).

Figure S5 (related to Figure 5)

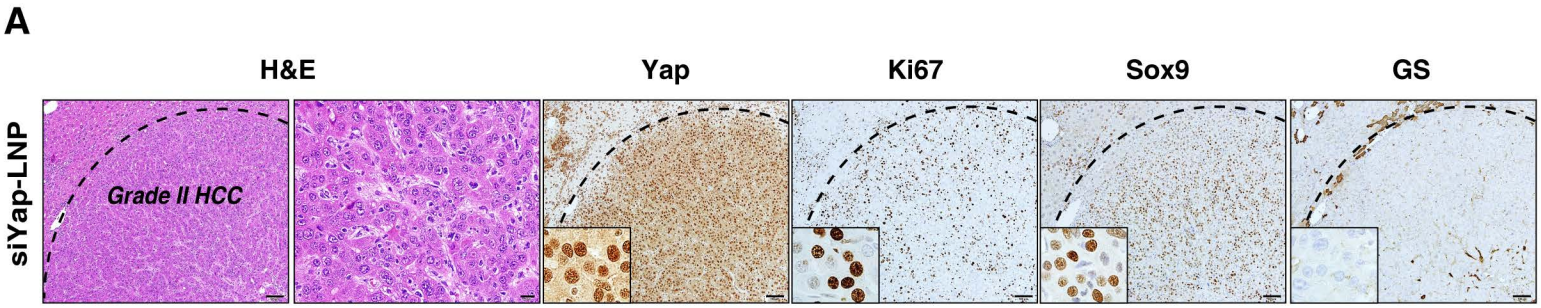

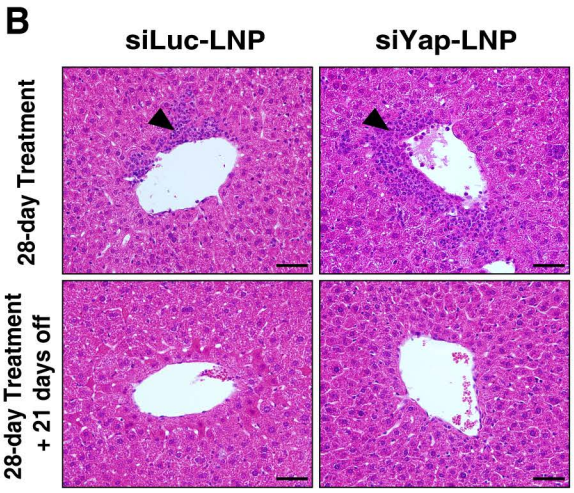

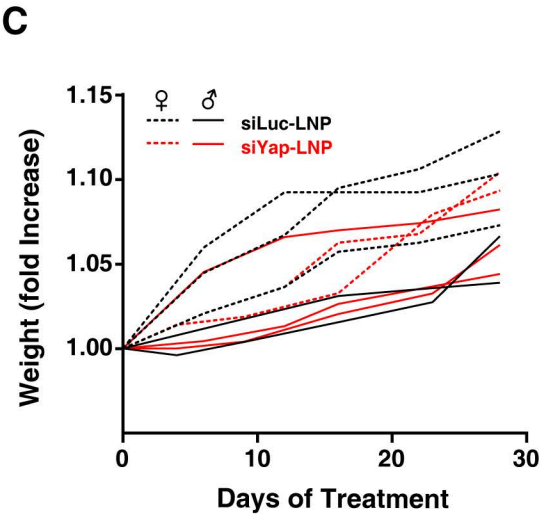

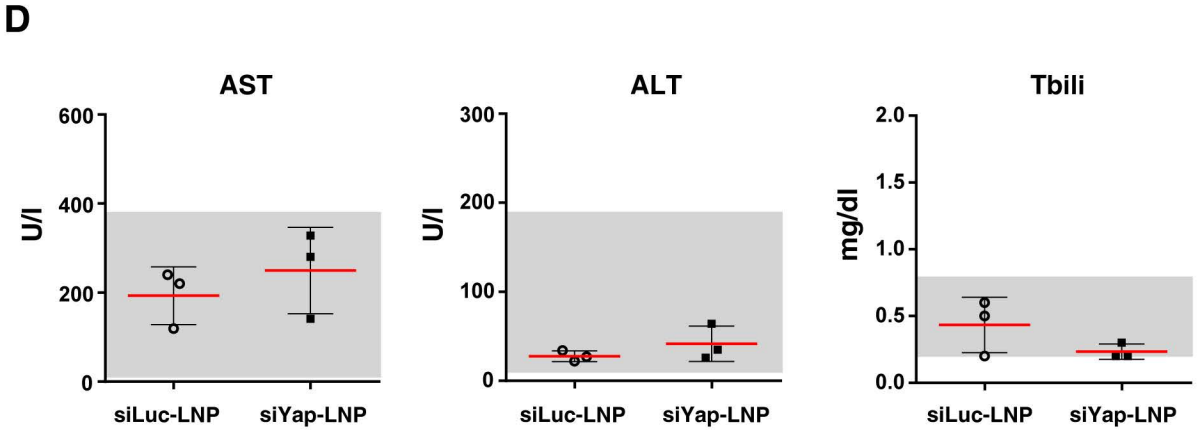

Figure S5. Response to long-term administration of siLNP formulations (related to Figure 5).

(A) While siYap-LNP treatment for 28 days greatly reduced the tumor burden in DKO mice, rare HCC foci were observed. Representative images of a resistant tumor are shown. These resistant tumors were high grade HCC that remained strongly positive for YAP, had high a level of Ki67 staining and expressed SOX9. Scale bar: 100 μm (H&E *left panel*, Yap, Ki67, Sox9, GS) and 20 μm (H&E *right panel*).

(B-D) Impact of siLNP treatment on liver function in WT mice. B) Representative H&E stained section showing a moderate inflammatory reaction (arrow heads) following 28 days treatment with the indicated siRNA-LNP formulations (*upper panels*). Inflammation was resolved within 3 weeks following discontinuation of the treatment (*lower panels*). Scale bar = 50 μm. C) No weight loss was observed during the course of treatment. D) Treatment with the indicated siRNA-LNP formulations for 28 days does not result in significant liver toxicity as reflected by normal levels of serum Aspartate Aminotransferase (AST), Alanine Transminase (ALT) and Total Bilirubin (Tbili). The grey areas indicate normal range of serum concentrations for the indicated factors.

Figure S6 (related to Figure 6)

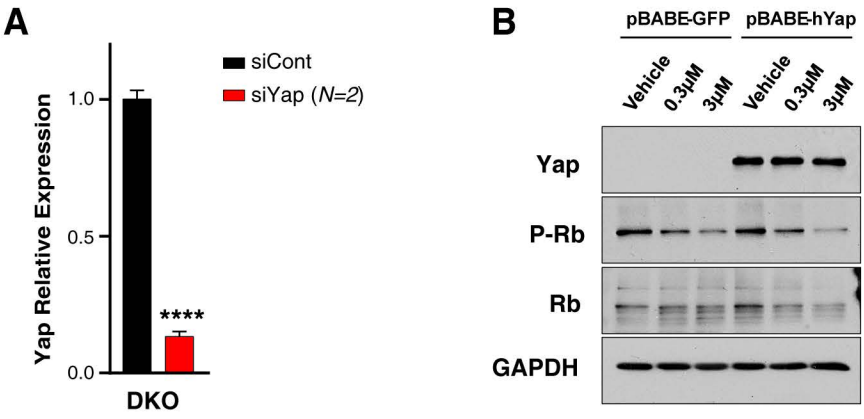

Figure S6. Modulation of *Yap* expression primary HCC cultures from DKO GEM model (related to Figure 6).

(A) qRT-PCR analysis of *Yap* levels in DKO cells 4 days following RNAi-mediated *Yap* knockdown. N= number of independent cell lines tested. Error bars indicate S.E.M. ****p<0.0001.

(B) Immunoblot analysis for YAP, phospho-Rb (p-Rb), Rb and GAPDH proteins of GFP-infected and hYAP-infected TKO cells treated with the CDK 4/6 inhibitor, PD-0332991, at the indicated concentrations.

Figure S7 (related to Figure 7)

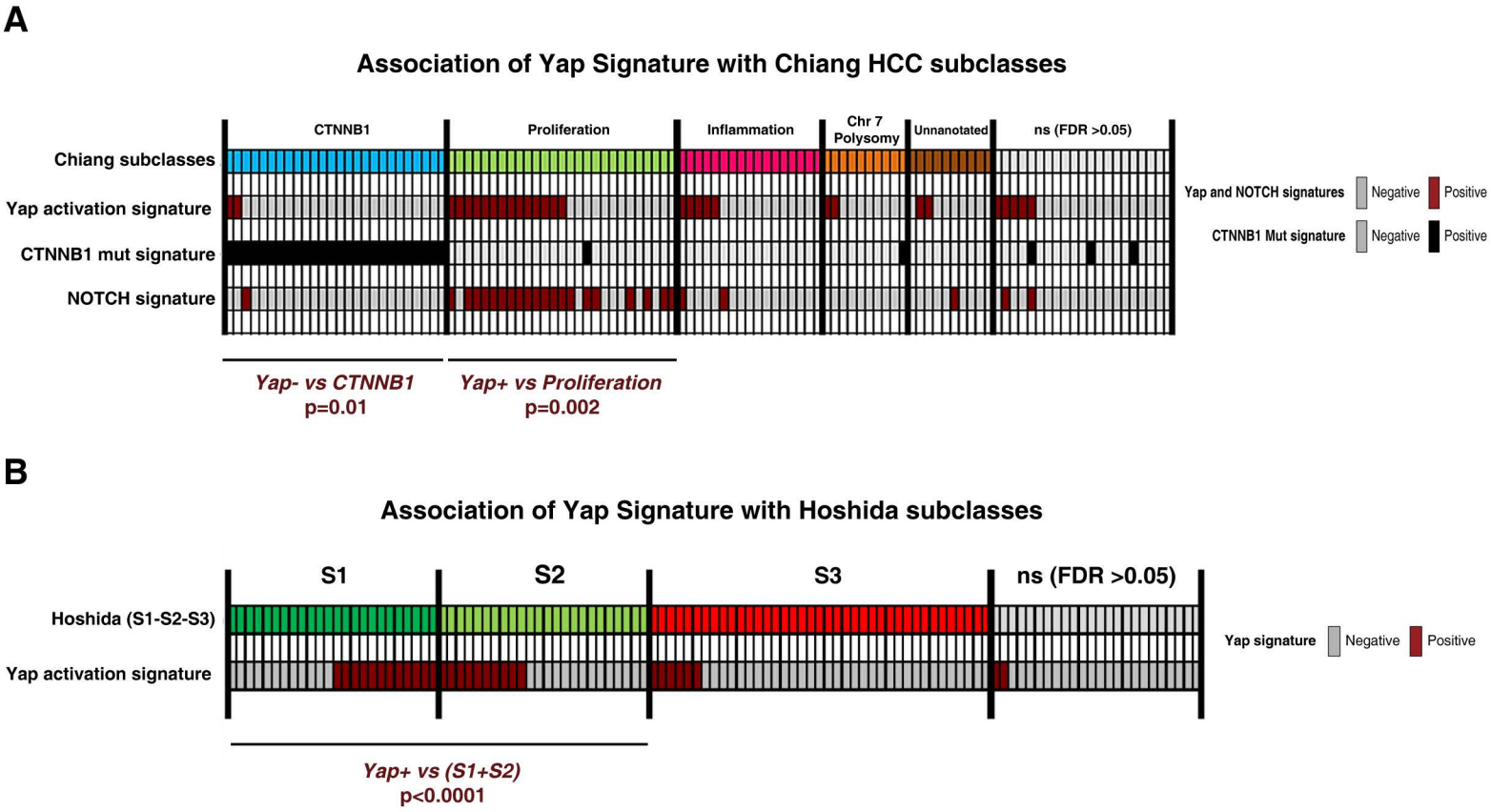

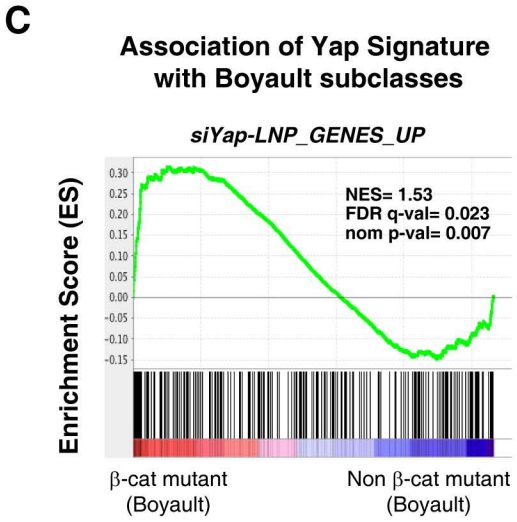

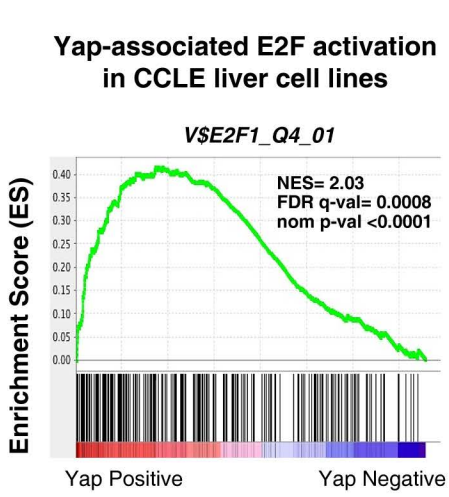

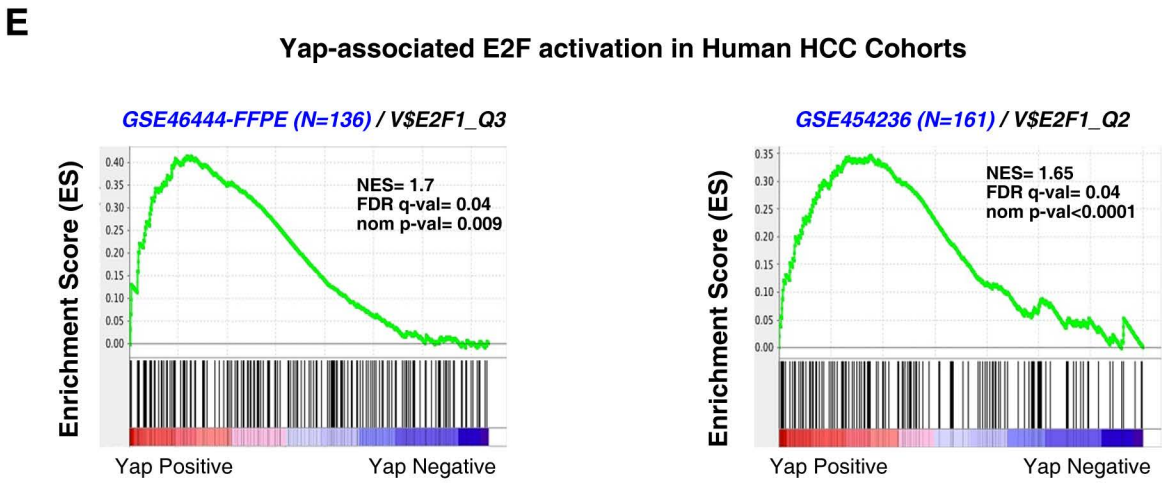

Figure S7. Association of Yap signature with distinct molecular subclasses of human HCC (related to Figure 7).

(A) Distribution of the YAP-activated (Yap+, red squares) and YAP-non activated (Yap-, grey squares) HCC samples according to the Chiang molecular classification (Chiang et al., 2008). Fisher's exact test was used for statistical analysis.

(B) Distribution of the YAP-activated (Yap+, red squares) and YAP-non activated (grey squares) HCC samples according to the Hoshida molecular classification (Chiang et al., 2008)

(C) Gene set enrichment analysis showing a positive association between the expression profile of siYap-LNP treated HCC (day 9) and the β-Catenin mutant human subclass according to Boyault classification (Boyault et al., 2007).

(D) YAP levels show significant correlation with an E2F signature in human HCC cell lines.

(E) YAP levels show close correlation with E2F signatures across two independent human HCC cohorts (N= 136 and 161 samples respectively).

Table S1 (related to Figure 2)

DKO^{Ad} DOWN	p-value
CCND1	3.00436E-05
XRN2	5.58099E-05
LZIC	5.72416E-05
EIF2AK2	6.43385E-05
MAST2	7.68621E-05
GEMIN6	9.58697E-05
VDR	0.000102549
RNF135	0.000116349
TUFT1	0.000128042
PDGFA	0.000161875
LY6E	0.000167352
AKAP2	0.000223971
SLC1A1	0.000236659
ILF3	0.000396038
TSPAN3	0.0004561
GTF3C5	0.0005623
ZBTB45	0.000601761
DPM2	0.00061727
APAF1	0.000666951
PGS1	0.000751706
SDC1	0.000772755
CAPN5	0.000783393
ANXA2	0.000845232
SYNPO	0.00085328
YAP1	0.000871184
SLC1A4	0.000929688
PFDN4	0.000980193
ANXA5	0.000995322
MRPS18B	0.001052865
THUMPD3	0.00106885
IRF9	0.001103467
ACSL5	0.001284578
LYVE1	0.001317042
DNM1L	0.001441476
INHBA	0.001462636
ANAPC4	0.00146873
STX18	0.001497477
SCAND1	0.001539366
NEDD9	0.001543404
IFIT2	0.001617072
TPD52	0.00166387
PAWR	0.001737249
KLHDC4	0.001760961
AHNAK	0.002117699
GPX4	0.002220399
SAE1	0.002261061
SEMA6B	0.002350212
FKBP1A	0.002411208
CEP170	0.00241953
EEF1E1	0.002427586
SLC25A30	0.002455156
JUN	0.002530054
PIP5K1C	0.002550501
RAB11B	0.002612557
NRG1	0.002699048
PLEKHA1	0.002726278
AGPS	0.00279152
TES	0.002844879
DPH3	0.002924009
CAT	0.002969132
ZFP36L1	0.002980624
CTPS	0.003002011
GARS	0.003095445
CPNE8	0.003177079
LRP10	0.003190938
UMPS	0.003294642
RPL30	0.003417663
LRRC20	0.003440713
KLF6	0.003561323
PKIG	0.003564917
RUVBL1	0.003657449
E2F6	0.003729686
SPECC1	0.003772431
NR2C2	0.003849316
PLEKHM3	0.003889726
TUBB2B	0.003971109
OSGIN1	0.004060284
LUZP1	0.004310483
LRRC59	0.00465436
CXADR	0.004678894
AGPAT9	0.004720753
TGM2	0.004731276
SLCO3A1	0.004852836
TNFAIP3	0.004928845
YWHAH	0.004988197
NID1	0.00500232
MITD1	0.005051648
LSM5	0.00510176
SNRPD1	0.005261496
HN1	0.005266291
RPL27	0.005321378
ETS2	0.005363808
LMNA	0.005505706
HIP1	0.005531055
IER3	0.005597788
LCMT1	0.005613236
SRP54	0.005742333
CORO1C	0.005763633
TSC22D1	0.005810612
WRB	0.005893372
MLF2	0.006280623
FZR1	0.006363208
MAP1LC3A	0.006385289
RGS5	0.006411841
FEZ2	0.006441337
AP1S1	0.006467902
SESN3	0.006518821
GIPC1	0.006698746
LASP1	0.006770986
WWC2	0.006783559
RPAP1	0.006788036
GRK5	0.006802141
CDKN1A	0.006852364
WARS	0.006936829
BMPER	0.006939158
ARID5B	0.00696466
MYL6	0.007176991
TMEM171	0.007264989
ANKRD40	0.00734295
KRT18	0.007450791

DKO^{Ad} UP	p-value
PIGU	3.22229E-06
F11	1.61889E-05
HGFAC	6.6176E-05
CCS	6.61971E-05
AHCY	6.73411E-05
KHDRBS3	6.99991E-05
IGFBP4	0.000127741
GNE	0.000155211
ZMYM5	0.000163598
SIRT2	0.000202935
TNXB	0.000268581
PLG	0.000273489
HAL	0.000282435
DIDO1	0.000318379
CPSF4L	0.000329504
PI4KA	0.000343235
COBLL1	0.000366363
IGFBP2	0.000369458
CPS1	0.00040211
UPP2	0.000422699
AGT	0.00042465
DNTTIP2	0.000426653
APEH	0.000432805
SP5	0.000449536
IL1RAP	0.00048104
SAA4	0.00049241
MARVELD1	0.000544783
PTPRD	0.000566194
ATP5SL	0.000701482
CRYL1	0.000755562
PANK1	0.000758529
MYH7	0.000774664
EIF2AK1	0.000785839
SMARCD2	0.000802124
SLC1A2	0.000860952
DMXL1	0.000875406
SCNN1A	0.000917815
IPO8	0.001046854
ABCG8	0.001069905
MPND	0.001101507
NQO2	0.001105437
SLC43A1	0.001216194
CTDSP2	0.001294638
TSHZ1	0.001323658
SEH1L	0.001328607
SSFA2	0.001396253
PIPOX	0.001406095
ARIH2	0.001441661
PAH	0.001445045
PROC	0.001512037
SAA2	0.001582043
FGF1	0.001590431
NIT2	0.001681589
FBXO9	0.001798203
RSBN1L	0.001894316
EPAS1	0.001919427
UGT1A1	0.001944783
SAA1	0.0019644
MLL3	0.002030902
SEPHS2	0.002039681
ANG	0.002151653
ERRFI1	0.002184767
DGAT2	0.002219788
HBS1L	0.002231165
VPS13B	0.002263236
RP9	0.002315709
SFXN1	0.002350792
MRPL48	0.00239175
CAPN8	0.002531792
HPD	0.002559345
NNMT	0.002577826
ZKSCAN1	0.002581041
SPATA2L	0.00259902
ITPR2	0.002624039
DPP4	0.002628617
SLC7A2	0.002681481
ASGR1	0.002701917
PRG4	0.00274827
RNF103	0.002860305
SLC17A2	0.002888745
MAOB	0.002888862
TPST1	0.00292272
CRCP	0.003019824
UQCRC1	0.003020765
USP28	0.003025731
ANPEP	0.003148293
HAAO	0.00321549
SMPD1	0.00321639
TOP1	0.003261716
LIN7A	0.003356315
CLMN	0.003547364
LDHD	0.003563619
SLC29A1	0.003570869
ITPR1	0.003613401
LMF1	0.003628018
LIAS	0.003737988
PROZ	0.003740492
KIF1B	0.003767107
KLF9	0.003773554
AATK	0.003937416
HEATR5A	0.004045751
PIK3CB	0.004141343
CAND1	0.004222987
ALDOB	0.004252646
VKORC1	0.004357393
CYP27A1	0.00436202
NDST2	0.004511071
FABP1	0.004592018
MOCS3	0.004631551
GPLD1	0.004668121
UBR5	0.004672722
SLC16A10	0.004797213
CES3	0.004818226
CHD9	0.00488248
COL1A1	0.004892834
TRIM23	0.004896639
TAT	0.004899049
RELN	0.004932384
ST3GAL5	0.005083568
TGFBRAP1	0.005155038

DKO^{Ad} DOWN	p-value
OSR1	0.007621908
CYR61	0.0076631
BCL2	0.007679706
SMYD5	0.007800395
ASB2	0.007862944
AMOTL2	0.007888838
ASAH1	0.007896257
RAP1B	0.007925303
RCAN1	0.00795259
EIF6	0.008047211
FBXL5	0.008122387
ARHGAP1	0.008246823
MAX	0.008255333
PPP1R11	0.008312894
PRMT5	0.008332423
NUDT5	0.008350278
SSU72	0.008353696
CDC42EP2	0.008369984
SGCB	0.00844192
RRAS	0.008700704
IRAK3	0.008710194
TMCO6	0.008719774
TPM1	0.008724417
PRDX6	0.008823526
LIMS2	0.008839035
CYBASC3	0.008963184
GPC3	0.008984243
TRADD	0.009046257
ZFP64	0.009064411
WWC1	0.009258044
FAS	0.009447678
FRMD8	0.009597289
PSMF1	0.009725106
NUP43	0.00973134
SOX9	0.009847731
FRMD4A	0.009979742
ATP8B4	0.010052371
IPO5	0.010148873
PNKP	0.010184851
ID1	0.010246108
IMP4	0.010298264
RPL18	0.010335191
TRAPPC4	0.010404867
RNF11	0.010491086
G3BP2	0.010623544
HP	0.010642739
KRAS	0.010649418
FBXO44	0.010787046
DEXI	0.010957812
THG1L	0.01098264
ABCC1	0.010984318
PPARG	0.011093101
LRP11	0.011319511
AQP8	0.01170701
TMEM184B	0.011751788
INSL6	0.011767227
RALB	0.011808457
POU3F3	0.011819963
TIMM17A	0.011859508
TJAP1	0.011891381
CDC7	0.011951452
WDR70	0.012042373
UBE2E2	0.012221488
STK38	0.012261699
DNMT3B	0.012297311
IER5L	0.012364502
SET	0.012465072
MED11	0.012487304
CCDC86	0.012530354
RAP2B	0.012615858
SNX6	0.012689988
AIG1	0.012723873
EEF1G	0.012760568
PRKAR1A	0.012955237
PSMA5	0.013008275
PTPN6	0.01308533
SERPINA7	0.013136281
MRPL11	0.01315835
ARRB1	0.013164674
NT5C	0.013223074
GRWD1	0.013285413
GDPD1	0.013342146
SOCS3	0.013412652
IL7	0.013497819
TJP3	0.01352133
ZNFX1	0.01355252
SLC16A5	0.013834843
BICC1	0.014168529
GGPS1	0.014204335
MDH1B	0.014329021
DUSP3	0.014332805
CEBPG	0.014395459
TGIF1	0.01448153
NUP93	0.014507408
SH3BP5L	0.014514236
ACTB	0.014525209
CHCHD4	0.014644873
PKP4	0.014709071
RPP30	0.014722155
CHD8	0.014822086
PANX1	0.015079533
CACNG4	0.015380666
PLRG1	0.015430359
ZMAT5	0.015440253
BMPR1A	0.015800036
PPL	0.015827368
MCM7	0.016005899
PPP2CA	0.016179726
NUDT18	0.016197186
SKIL	0.016322563
GSTA2	0.016366787
SOAT1	0.016457909
MED24	0.016475364
RPS6KL1	0.016808991
DMBX1	0.016854669
SERPINA5	0.016939174
FBLN2	0.01706379
E2F2	0.017324323
PSMD7	0.017332036
CFL2	0.017484675

DKO^{Ad} UP	p-value
ASGR2	0.005176787
MLXIPL	0.005191494
AIM1	0.005262345
ZMIZ2	0.005291606
MCCC2	0.005367172
FBXO31	0.005400349
ARSB	0.005495023
PIM3	0.00553052
FCAMR	0.005607643
KIF13A	0.00561224
PAPSS2	0.005779463
LPIN2	0.00586598
WIPI1	0.005868143
CUX1	0.005880728
PCCB	0.005881338
C8B	0.006108761
SLC20A2	0.006147432
PCK1	0.006173989
HELB	0.006206894
TLE1	0.006315864
CAMTA1	0.006473292
ADH5	0.006632524
MFSD1	0.006751354
GALNT14	0.006786737
IFT52	0.006789927
PRR3	0.006853473
GPHN	0.006909625
SERPINA6	0.007015856
GSTT1	0.007142861
SLC2A9	0.007217078
CLK3	0.007242574
AFMID	0.007254328
AS3MT	0.007296513
DYNLRB1	0.007308999
DBT	0.007361198
ABCD3	0.007425092
C8A	0.007443282
PDHA1	0.007518416
ABHD3	0.00755309
HNF4A	0.007560613
KLHL21	0.007578458
THSD1	0.007634061
COX7A2L	0.0077354
OCLN	0.007815237
TMEM201	0.00796862
PCP4	0.007999179
AMDHD1	0.008007591
AK3	0.00802113
USP54	0.008036207
MRPS27	0.008287581
CTDSPL	0.008300509
SARDH	0.008312182
AGPAT6	0.008385901
PARP16	0.008620559
CYP17A1	0.008636778
COASY	0.008715807
SAFB	0.008723646
SLC6A12	0.008815195
VAC14	0.008831359
DLAT	0.008854003
ATP13A3	0.008865782
USP47	0.0089759
GBE1	0.009142395
EGFR	0.009269734
ASAH2	0.009398053
SERPINF2	0.009434913
PRR16	0.009603879
EIF4G2	0.009740579
SEMA6A	0.009965667
NPC1	0.009983175
HECTD3	0.010047937
CUL4A	0.010090873
ENPP6	0.0103073
AP3M1	0.010365501
ENPP2	0.01046969
FCGR2B	0.011004562
SLC2A2	0.011056609
FURIN	0.011120671
IRF2	0.011155296
PTGIS	0.01116416
ACSF3	0.011294811
PDZK1	0.01131015
MORF4L1	0.011371159
TNR	0.011453094
ANKRA2	0.011455816
FOXN3	0.011463914
SMCR7	0.011501679
FETUB	0.011564646
ARHGAP26	0.011577917
GLRX3	0.01164205
MYLK	0.011712096
UVRAG	0.011733571
SEPP1	0.011908251
GHR	0.011920398
ECM1	0.012008756
LRPPRC	0.01228903
SOX5	0.012324891
MCTS1	0.012344497
MOCS2	0.012351303
SFXN5	0.012705846
ACSL1	0.012971088
STARD10	0.013386948
TNRC6C	0.013450099
RAD17	0.013495516
OSGEPL1	0.013497491
SYT1	0.013616192
TAOK1	0.013946748
BCAS3	0.013991015
ZFAND2B	0.014111552
ZMYND11	0.01419419
ZCCHC8	0.014295203
ELL2	0.014349933
ETNK2	0.014362416
BMF	0.014374092
PITPNM2	0.014451199
ABCA9	0.014512889
PKN2	0.014545505
ADIPOR1	0.015094677
HTRA4	0.015169438
GATAD2B	0.015218582

DKO^{Ad} DOWN	p-value
RBPMS	0.017603328
NEDD8	0.017638899
CSDA	0.01764718
NT5E	0.017655665
HOXD1	0.017686024
ELF3	0.018094791
NGFRAP1	0.018133444
PPIA	0.018163422
MTA3	0.018184785
EPS8L2	0.01821639
RPL32	0.018244478
PLSCR1	0.018917
NSMCE1	0.019011385
GPRC5B	0.01908257
RPL24	0.019142913
CYGB	0.019173675
LAMC1	0.019292714
CAMSAP1L1	0.019458862
SORL1	0.019667852
PGD	0.019678578
HNRNPC	0.019881286
SH3PXD2B	0.019893654
NME4	0.019916954
TBC1D12	0.019970487
RALY	0.019995489
PFN1	0.02021477
TPX2	0.020367883
CDKN2AIPNL	0.020425035
CAST	0.020474751
NAIF1	0.020557248
SRGAP2	0.020580174
CREB3	0.020719399
BMP4	0.020859639
UBTD2	0.020904745
NFE2L2	0.020970013
P2RY14	0.020996517
SYS1	0.021011023
DNAJC7	0.021090438
TINAG	0.021154822
GCA	0.021412597
CLIC4	0.021503623
ZC3HC1	0.021528143
ADORA2B	0.021643503
ITGB3BP	0.022003964
ABI3	0.022030919
FGFR1OP2	0.022191833
SLC16A6	0.022220522
HSPBAP1	0.022429297
GTPBP3	0.02243924
PACSIN3	0.02250077
MAPK4	0.022640164
HDHD3	0.022655849
ZCCHC6	0.022825902
PLAU	0.02291216
SLC40A1	0.023065614
GDF15	0.023614824
SYT8	0.023958976
LBH	0.023962348
PSMA2	0.024118584
IL1A	0.024419647
TMEM55A	0.024440925
FOSL2	0.024581669
PPP2R5D	0.024589923
PLOD3	0.024867317
CCNG1	0.02498182
STAP1	0.024983988
AP1M1	0.025013018
OBFC2A	0.025101777
PDPK1	0.025225305
ID3	0.025586589
PICK1	0.025751323
SP100	0.025878061
CCDC126	0.026043225
DDI1	0.026071322
SRI	0.026651092
ZC3H3	0.026712423
VPS37B	0.026741915
RRP1B	0.026914388
ITIH5	0.026916911
WDFY1	0.027080706
PALLD	0.02727725
PCGF5	0.027418658
ORAOV1	0.027504541
AP2S1	0.027776482
OXGR1	0.027911374
MARCKS	0.028223016
SPATA17	0.028255414
TLE3	0.028444503
NXN	0.028858821
LARS	0.028905467
PLTP	0.029441567
DAB2IP	0.029530604
TBC1D20	0.029731173
ATXN2L	0.030025264
LRCH1	0.030095735
PRDX3	0.030174153
AGR3	0.030263986
KRT8	0.030344451
ZEB2	0.03037863
SNX10	0.030708167
ICK	0.030711319
CLDN6	0.03077096
ALOXE3	0.031024877
FLVCR1	0.031238502
PVR	0.031452434
MANBAL	0.031478321
TBC1D22A	0.031513579
CCDC23	0.03165858
ATP9A	0.03177811
DHCR24	0.031851367
ANKRD1	0.031966874
GSTA1	0.032027285
TMEM160	0.032535039
LHFP	0.032540864
ADAM17	0.032624097
EVI2A	0.033000992
EMCN	0.03339773
BTBD11	0.03360049
COX19	0.033774626
EIF2B3	0.033787629

DKO^{Ad} UP	p-value
ENTPD4	0.015299523
IREB2	0.015402902
TLCD1	0.015619375
C2CD3	0.015635697
SMARCC2	0.015812797
BRAF	0.01586777
TAPT1	0.015920228
KIF21A	0.016024041
KISS1	0.016192191
SCAP	0.016293399
ATP1B1	0.016388604
ABAT	0.016537167
CDC14B	0.016633398
MAT1A	0.017172358
FANCE	0.017195869
ACOX1	0.017199198
SPATA5L1	0.017258387
XDH	0.017275582
TRAK1	0.017337501
SLC38A2	0.017645739
SSBP3	0.017658599
ALDH1L1	0.01766071
CGRRF1	0.017828934
GGNBP1	0.017850761
SAR1B	0.018284609
SCYL1	0.018326573
STK3	0.018486942
SLC45A1	0.018568992
NOTUM	0.01859301
GAPVD1	0.018675608
ANXA11	0.018733548
POR	0.018767953
BBOX1	0.019018661
SLC25A25	0.019036608
STIM1	0.019377269
MIER3	0.019589016
ZWILCH	0.019610543
AGPAT5	0.019637523
ETFA	0.01998751
PYGL	0.020026603
LMAN2	0.020218507
TEF	0.020225653
RFC1	0.020469737
SCNN1B	0.020626636
TMEM146	0.020921886
FKTN	0.020944465
ALB	0.020953622
WDR3	0.021135733
APOB	0.021340825
TBX3	0.021451671
PARD3	0.02149964
MAPK6	0.021506002
SMOC1	0.022095198
ZDHHC14	0.022315142
XPR1	0.02236684
DIS3L2	0.022425967
TMEM100	0.022874222
ADI1	0.023109812
FGL1	0.023238917
CPNE1	0.023557306
SFT2D2	0.024043506
ZHX3	0.024294648
KYNU	0.024318458
B3GALT1	0.024364011
TARDBP	0.024452873
AKAP9	0.024489664
TK1	0.024625703
RTP2	0.024889412
ALDH1B1	0.02511162
APH1A	0.025121989
APOA2	0.025325482
RCL1	0.02538368
DAZAP1	0.025536909
FLNB	0.025560388
ITGA1	0.025603724
POLB	0.025873062
DEPDC5	0.026153107
AFF1	0.026382968
ACO2	0.026679126
CREBL2	0.026913524
AQP4	0.027004876
RTN4IP1	0.027199304
CPB2	0.027361349
GJB1	0.027449677
RUFY1	0.027619657
SMG7	0.027751059
ASL	0.027883862
PDHB	0.027960379
FGB	0.027990128
MBD5	0.028306982
RHOBTB1	0.028319021
SMYD2	0.028492944
STS	0.028767658
STAB2	0.028882205
ONECUT2	0.028985844
GLYCTK	0.028988973
GALM	0.029046253
NDRG3	0.029097669
SLC47A1	0.02923274
NEK9	0.029288869
SHANK2	0.02935771
NEB	0.029703853
HDAC11	0.029934114
MYO1B	0.030222735
SORD	0.03033099
GTF2I	0.030353377
CENPL	0.0303815
FBLN1	0.030400854
ECE1	0.030439677
DKK4	0.030503493
YIPF4	0.03050554
KLF13	0.030680635
PRPSAP1	0.030698715
IL13RA1	0.030830962
TMED2	0.030840701
THNSL2	0.03100391
LTBP4	0.03103648
USP16	0.031084154
HGD	0.031272152
COBL	0.031379597

DKO^{Ad} DOWN	p-value
KLHDC2	0.034331416
SLAMF9	0.034332501
LMCD1	0.03436566
TMEM181	0.034412826
RNF148	0.034543811
RPL9	0.034630006
TMEM51	0.034642624
GALNT1	0.03466252
PSMC5	0.034776527
PRR13	0.034814504
EDEM2	0.034893268
PKP2	0.034985932
C1GALT1	0.035322932
ADSS	0.035372342
TLL1	0.035373787
NEDD4L	0.035501732
SORBS2	0.036249208
PACSIN2	0.036670836
OSBPL3	0.036875168
NPTN	0.037128741
SOX4	0.037381299
ZNRD1	0.037388567
PAX8	0.037754206
CLDN10	0.037790393
FSD2	0.038260963
PEF1	0.038604656
IL33	0.038713559
RETN	0.038989956
TCEA1	0.039028439
HDC	0.039669747
RND2	0.039679603
FANCA	0.039731806
CLDN9	0.039763416
SDCBP	0.039838563
SERPINB8	0.039879016
RCE1	0.039999138
CYP1A1	0.040064486
PLCG2	0.040253941
PSCA	0.040295549
UTP11L	0.040373771
KRT23	0.040720413
ODC1	0.040816914
CAPN51	0.040982938
MOBKL2B	0.041046879
CBX5	0.041210172
DHX38	0.041295475
ELMO1	0.041354209
CLDN5	0.041477828
BMPR1B	0.04163136
SNX2	0.041812302
NPSR1	0.041827362
MRPS23	0.04192004
PDCD10	0.041968213
SMOX	0.041968341
AMN	0.042373744
GATM	0.042621984
KSR2	0.042662673
DNAJC17	0.042676773
RTP4	0.043458502
TNFRSF10B	0.043483471
ITPR3	0.043599494
CCDC92	0.043647173
INSM2	0.043744759
MAPK3	0.043968585
RPL7L1	0.044291753
ABTB2	0.044958177
CLIP2	0.045073375
LSM12	0.045567839
MYH9	0.045739747
MKI67IP	0.046627742
CELSR3	0.047126257
INTS12	0.047169326
PKP3	0.047287106
EMP2	0.047507731
GNB1	0.047563925
LAMC2	0.04775349
FGFR1	0.047793443
CHMP4B	0.047961287
CCDC56	0.048077234
KLHL14	0.048233052
GTF2E2	0.048371818
CAPZB	0.04838724
ORMDL3	0.048899632
ARPC5	0.048971534
ACOX2	0.049108901
ZCCHC4	0.049514331
ATP7B	0.049777143
SLC7A11	0.049833083
SLC4A4	0.04990819
PDLIM1	0.049944596

DKO^{Ad} UP	p-value
FZD2	0.032102188
ARG1	0.032246179
NGEF	0.032319404
FRAS1	0.032371525
IGF2AS	0.032500393
MUC2	0.032553662
HECTD1	0.032712889
DST	0.032942031
SNX29	0.033105317
CHD4	0.033146862
SLC39A14	0.033226424
CTNNBIP1	0.033240014
ACBD4	0.033264439
TFPI	0.033296433
SLC12A7	0.03333193
TRPC4AP	0.033348297
PGRMC2	0.033547661
DGKH	0.033577959
HNRPDL	0.033653922
PHF17	0.033926647
CPT2	0.034030417
ABHD13	0.034044686
POLE4	0.034095781
SLC6A16	0.034281285
ABCA8	0.034389368
LPIN1	0.034494238
IQGAP2	0.034870611
HBP1	0.034891845
G6PC	0.035141487
RBM22	0.035823059
ZZEF1	0.035833727
CTLA4	0.036003701
SOX6	0.036106931
MTHFR	0.036128792
AMIGO2	0.036172319
POLG	0.036181295
EPC1	0.036346883
USP35	0.036696088
LRIG1	0.03677777
PSMB5	0.036856965
LGR5	0.036907818
CACNA1D	0.037030303
PANK3	0.037122603
CTAGE5	0.037246953
TIMP2	0.037252506
CCDC88A	0.037347205
SLC25A15	0.037609623
FAH	0.037731415
GOLIM4	0.037758411
CHST4	0.037779548
DDAH1	0.03780851
DTNB	0.038002607
DHTKD1	0.038082497
SUSD4	0.038573752
RPAIN	0.038580094
LANCL1	0.03865226
HSPA12B	0.038745907
HLCS	0.038793853
GNA14	0.039157898
SREBF1	0.039376961
STX6	0.039833649
TCEB3	0.040120907
PYGB	0.040303623
CD82	0.040572695
SEC61A1	0.040632958
GIN1	0.040666725
SPG7	0.040761603
APBB2	0.041253191
LONP2	0.041387991
SMARCA2	0.04149745
MAP2K3	0.041750206
SYNGR4	0.04190646
YPEL3	0.04205487
PPP1R10	0.04208679
EML1	0.042570494
ZFYVE26	0.042846555
TACC1	0.043184205
SMURF1	0.043248852
DUOXA1	0.043917866
RANBP9	0.0439626
MAPK14	0.043974299
ZDHHC6	0.044412554
MAP2K7	0.044546953
NCOA4	0.044807175
STAG1	0.044930387
ACSM1	0.045338302
MRPS35	0.045704345
FGA	0.045709357
RBKS	0.045883004
KIF20A	0.046306658
FGD6	0.046641241
SERPINE2	0.046663824
POLR3A	0.046878056
IL18	0.047068996
SND1	0.04748409
RAB11FIP3	0.047706806
SLC17A5	0.047869226
UBP1	0.048191558
ACOT12	0.048214362
CHN2	0.048286036
HSD17B6	0.048390921
SETX	0.048409728
SARM1	0.048453626
VAPA	0.048508415
EEA1	0.048564298
PLOD1	0.048567741
CPVL	0.049602071
LMO7	0.049688165
GCKR	0.049825025

Table S1. Predicted direct Yap targets following Mst1/Mst2 DKO (related to Figure 2).

Gene set based on the integration of differentially expressed genes following acute activation of endogenous YAP (DKO^{Ad} versus WT^{Ad} livers at day 8) with chromatin immunoprecipitation data for TEAD binding sites in hepatic cells (ENCODE database) (see also **Fig. S2B**). Genes are ranked based on p-value.

Table S2 (related to Figure 4)

siYap DOWN	Fold Change (siYap/siLuc)	q-value
TMIGD1	0.017605866	0.00340081
SLC22A7	0.021711753	0.000493027
PTPRH	0.029833768	0.0282462
AFP	0.046853155	0.000493027
SLC44A4	0.055979406	0.000493027
PLCH1	0.056940146	0.000493027
KLHL31	0.060358468	0.000493027
GUCA2A	0.064628755	0.00169137
IGFBP6	0.065423375	0.000493027
SLC19A3	0.069147936	0.00488988
SHBG	0.073301676	0.000493027
APOA4	0.078827345	0.00488988
GGT1	0.081555727	0.000493027
PLCB4	0.102844033	0.000493027
SLC7A11	0.106175293	0.000493027
AIF1L	0.111704561	0.00401827
PCYT1B	0.116960233	0.000493027
DUSP9	0.127876228	0.000493027
HBEGF	0.136794298	0.000493027
GSN	0.140025356	0.000493027
ANK2	0.140224467	0.000493027
TMEM169	0.1495946	0.000493027
CPE	0.151652375	0.000493027
SLC3A1	0.1600739	0.00169137
DDR1	0.176553827	0.000493027
CLDN6	0.182483762	0.000493027
MOGAT2	0.189836591	0.000493027
SGCE	0.198105385	0.000493027
CRYL1	0.212355002	0.000493027
PDGFD	0.213114402	0.000493027
AMDHD1	0.21916814	0.000493027
FGFR2	0.221718337	0.000493027
TEAD4	0.236167116	0.000493027
TUBB2B	0.238961483	0.000493027
NTN4	0.240408532	0.000493027
SH3TC2	0.24474987	0.000493027
TUFT1	0.252282143	0.000493027
FAM154B	0.256487425	0.00340081
KIF20A	0.260717621	0.0420114
HSD17B6	0.261620954	0.000493027
GLIS3	0.263084836	0.000493027
TNFRSF12A	0.265469864	0.000493027
IL33	0.270730625	0.000493027
GAS2	0.270770036	0.000493027
CTNNBIP1	0.278434522	0.000493027
SESTD1	0.281900902	0.000493027
ESCO2	0.282274361	0.000493027
CKS1B	0.285699418	0.000493027
TMEM159	0.287168617	0.000493027
FKBP1B	0.292131533	0.00993221
STC2	0.304820112	0.000493027
LRRC1	0.305969552	0.000493027
CPS1	0.311069747	0.00131613
SLC20A1	0.318626905	0.000493027
CHEK1	0.318653409	0.000493027
DTNA	0.322032902	0.000493027
SERPINA5	0.322186958	0.00241048
TSPAN8	0.323545384	0.000493027
YAP1	0.327982331	0.000493027
LRP11	0.331396438	0.00401827
MGMT	0.331784869	0.000923837
SRC	0.332258958	0.000493027
EHF	0.332932127	0.000493027
ITGA6	0.339748715	0.000493027
GPC3	0.342650572	0.000493027
DTL	0.345661062	0.000493027
VWA1	0.348785024	0.00241048
GDPD1	0.349886765	0.000493027
SFXN1	0.353457828	0.000493027
PASK	0.356699228	0.000493027
PLEKHH2	0.360359804	0.000493027
AKR1D1	0.361811458	0.000493027
PDE7A	0.364805655	0.000493027
CEP57L1	0.365286413	0.000493027
HES1	0.36568415	0.000493027
SERPINF2	0.372690513	0.000493027
KNTC1	0.374892794	0.000493027
SDPR	0.375983173	0.000493027
POLR2L	0.377895698	0.000493027
KRT18	0.378561605	0.000493027
CASP4	0.379205028	0.000493027
PDZK1IP1	0.383226704	0.000493027
RRAGD	0.386475804	0.000493027
BBX	0.394648453	0.000493027
ITGAE	0.394719583	0.0164226
NUCB2	0.397021764	0.000493027
HAL	0.397492625	0.000493027
CCDC18	0.402142857	0.000493027
SH3BP4	0.403119646	0.000923837
CDKL4	0.405698536	0.0426939
PARD6B	0.408990716	0.000493027
CLDN1	0.409373608	0.000493027
SULT1A1	0.413557547	0.000493027
KIFC3	0.414835136	0.000493027
ASB2	0.415888875	0.0386244
CYR61	0.418500137	0.000493027
UROC1	0.418595875	0.000493027
PSPH	0.419566094	0.000493027
CLDN14	0.419958886	0.007639
IGFBP2	0.423073433	0.000493027
SMO	0.424542238	0.000493027
RCAN1	0.424954416	0.000493027
NCOA7	0.42539648	0.000493027
ADAP1	0.427670025	0.00131613
GPR56	0.428022932	0.00169137
KRT8	0.429574422	0.000493027
TBC1D30	0.434816924	0.000493027
ECT2	0.439757473	0.000493027
TOP2A	0.439931253	0.000493027
KYNU	0.441097656	0.000493027
TRIM35	0.442708813	0.000493027
FAM65C	0.443535043	0.0257279
KIF18B	0.448736363	0.0392456
FAM129B	0.44887013	0.00430332
KAZN	0.449259215	0.0128451
PLEKHA4	0.449857506	0.0350541
TCF19	0.450934564	0.00659163
SVIL	0.451456848	0.000493027
KIF2C	0.45277619	0.00603958

siYap UP	Fold Change (siYap/siLuc)	q-value
LGR5	90.38365539	0.000493027
NOTUM	80.67389461	0.000493027
AXIN2	56.47341618	0.000493027
SAA2	32.7592404	0.000493027
SAA1	29.96341177	0.000493027
NKD1	26.82097912	0.000493027
RNASE4	17.39318217	0.000493027
SLC25A21	16.0636741	0.000493027
ANG	15.72654662	0.00790866
PPP1R3G	15.62527851	0.000493027
NPR2	12.55465083	0.000493027
DUOX1	11.01410224	0.00307913
CREB3L1	10.74318602	0.0201176
SLC7A5	10.59373926	0.000493027
PDZRN3	10.25616875	0.000493027
RNF43	9.368967074	0.000493027
PLIN4	8.458196047	0.000493027
GPR110	8.454151699	0.000493027
TCF7	7.606379921	0.000493027
BCL9L	6.112404417	0.000493027
POR	5.991926803	0.000493027
MRVI1	5.079019454	0.000493027
TNXB	4.976598505	0.000493027
EFR3B	4.853784309	0.000493027
SLC17A1	4.709585203	0.000493027
SLC13A3	4.702115575	0.000493027
COL1A1	4.301798651	0.000493027
SLC38A11	4.299115887	0.0146108
MMP9	4.229567071	0.000493027
SLC25A25	4.21242208	0.000493027
DHCR24	4.183701728	0.000493027
SETD1B	4.041945867	0.000493027
ALDH3A2	4.037241812	0.000493027
USP2	3.991663208	0.000493027
INF2	3.873586617	0.000493027
ALAS1	3.818034132	0.000493027
IQGAP2	3.804429162	0.000493027
SCNN1A	3.794369035	0.012357
ALDH2	3.784125667	0.000493027
ZFHX3	3.761270331	0.000493027
SGK2	3.688821552	0.000493027
DPF3	3.687185502	0.00738558
ZNRF3	3.676186604	0.000493027
LEAP2	3.631536298	0.000493027
ASB4	3.625776507	0.000493027
UGT1A1	3.605251739	0.00868707
TBCEL	3.601754878	0.000493027
FASN	3.598535772	0.000493027
PDE4D	3.530493841	0.000493027
TEX12	3.494776029	0.0481952
SORBS3	3.49303234	0.000493027
GRHL1	3.457214219	0.000493027
C5AR1	3.412975363	0.00401827
MBL2	3.383907189	0.000493027
F11	3.317048255	0.000493027
SLC1A4	3.303373273	0.000493027
KHDRBS3	3.301496233	0.000493027
IL22RA1	3.274648372	0.000493027
SDR9C7	3.246713315	0.000493027
SAA4	3.23902589	0.000493027
AMACR	3.148926318	0.000493027
ZBTB45	3.055460859	0.000493027
NCOR2	2.992933035	0.000493027
INHBC	2.938378001	0.000493027
TAT	2.926365557	0.000493027
DOCK6	2.920165225	0.000493027
SLCO2B1	2.888458967	0.000493027
HMGCR	2.888038551	0.000493027
EFHD2	2.869680259	0.000493027
TUBB1	2.863421395	0.0352232
ATN1	2.860386303	0.00274527
PRRC2A	2.825546634	0.000493027
ACSF2	2.80288004	0.000493027
C2CD2	2.796902573	0.000493027
KDM6B	2.760366826	0.00241048
LPIN2	2.755778626	0.000493027
LRP1	2.748948731	0.000493027
MAP3K13	2.741508601	0.000493027
KLHL21	2.736155077	0.000493027
HYAL1	2.724213928	0.000493027
HMOX1	2.710483078	0.000493027
WDR91	2.70862374	0.000493027
COBLL1	2.707291061	0.000493027
SEMA3B	2.698859737	0.000493027
MTUS1	2.689466465	0.000493027
SRSF4	2.658679734	0.000493027
SERPINA7	2.652476556	0.000493027
PAH	2.61917054	0.000493027
AHCY	2.605445361	0.000493027
CORIN	2.590014186	0.00843096
RAB4A	2.578013824	0.00131613
IGFBP1	2.553683977	0.000493027
PTPRF	2.543967077	0.000493027
KIF1B	2.543103185	0.000493027
ACSL1	2.498755946	0.000493027
IL1R1	2.484025528	0.000493027
KLHL23	2.482218301	0.000493027
SETD1A	2.479535705	0.000493027
RIN3	2.473870532	0.000493027
NR1D1	2.469809896	0.000493027
HIPK2	2.45610119	0.000493027
SUOX	2.453055713	0.000493027
PANK1	2.450472574	0.000493027
PER1	2.439287825	0.000493027
VNN3	2.424302959	0.000493027
MERTK	2.416719442	0.000493027
WASF2	2.407507012	0.000493027
CHST15	2.406272449	0.000493027
STK40	2.404438457	0.000493027
LTBP4	2.404188475	0.00169137
FST	2.397831032	0.00868707
ROBO1	2.390728	0.000493027
PTDSS1	2.378743971	0.000493027
SLC9A1	2.372190712	0.00659163
TGM1	2.365229211	0.000493027
EXPH5	2.351905347	0.000493027
DHCR7	2.349493864	0.000493027
SLC25A45	2.329321858	0.000493027
FGL1	2.316874663	0.000493027

siYap DOWN	Fold Change (siYap/siLuc)	q-value
LAMB2	0.453181226	0.000493027
AGFG1	0.454691519	0.000493027
SALL2	0.459516955	0.007134
NSMCE1	0.460521367	0.000493027
MANSC1	0.460885409	0.0417107
CLU	0.46154397	0.000493027
S1PR2	0.466623218	0.000493027
RRM2	0.472992758	0.000493027
PARK2	0.475698704	0.00547498
GSTA4	0.476332206	0.000493027
RAD54B	0.478496408	0.0463954
CCHCR1	0.480827062	0.00993221
LIMS1	0.481077089	0.000493027
CENPF	0.481380631	0.000493027
PMS1	0.481711076	0.000493027
JAG1	0.486064609	0.000493027
COL27A1	0.486327474	0.00307913
CHEK2	0.488489684	0.00401827
ITPRIPL2	0.489035126	0.000493027
KIF20B	0.49179535	0.000923837
PLAU	0.492911314	0.000493027
AMOTL2	0.494392924	0.000493027
PTRF	0.49705934	0.000923837
PIGF	0.499463099	0.0450526
FAM115A	0.499847531	0.000493027
PPIL3	0.50309369	0.000493027
NEDD9	0.507047567	0.000493027
CTGF	0.507423415	0.000493027
STX6	0.507889305	0.000493027
WDPCP	0.507976619	0.00241048
ACOT6	0.513342994	0.0405843
SGOL2	0.513923312	0.00307913
RNF181	0.515760074	0.0192159
SERPINB8	0.516605533	0.00459373
RTKN	0.518626921	0.000493027
LLGL2	0.5194814	0.000923837
IER3	0.519907546	0.00816443
CCDC148	0.52148946	0.0362817
SNAP47	0.524331091	0.000493027
SKA2	0.525806543	0.0235792
TBC1D19	0.526842268	0.00131613
ATAD2	0.527111108	0.000493027
CEP19	0.527869421	0.00274527
APOM	0.528395103	0.000493027
LOXL4	0.528507189	0.0173577
PLD1	0.534437075	0.000493027
ICAM1	0.534630482	0.000493027
BMF	0.536083263	0.000493027
GRB10	0.539212931	0.00574126
RCN1	0.540774489	0.000923837
E2F1	0.540934568	0.028417
ORMDL1	0.541984313	0.000493027
FZD7	0.544076718	0.000493027
CASC5	0.544126501	0.00274527
CAPG	0.544591738	0.00430332
METTL21A	0.545034327	0.00169137
LIN7A	0.548624137	0.00131613
RANGAP1	0.550150407	0.000493027
GTPBP4	0.554842421	0.000493027
MAPKAPK3	0.555179422	0.007134
LDB1	0.556585411	0.00131613
G2E3	0.559880951	0.00169137
CCDC90B	0.56022606	0.00131613
GSS	0.560347229	0.000493027
UXS1	0.560605188	0.00307913
PKP4	0.561970771	0.000493027
SERPINA10	0.56518771	0.000923837
ANAPC4	0.567010753	0.000493027
ERGIC1	0.568916173	0.000923837
ANXA4	0.569475626	0.00131613
LAMA5	0.569725545	0.00241048
SDCCAG8	0.570786453	0.00206129
CAPRIN2	0.570816523	0.0302846
TINAGL1	0.571885408	0.0271157
FRY	0.573686709	0.00241048
MCM7	0.575572672	0.00206129
TPX2	0.576477817	0.0130893
TLCD2	0.579037625	0.00241048
PRRG1	0.580098583	0.0164226
ID2	0.580142011	0.000493027
TRMT11	0.580222441	0.00371096
ATP1B1	0.581390741	0.0181714
GRWD1	0.583068383	0.0371047
MITD1	0.583585119	0.00738558
MYL12A	0.585375796	0.00169137
ITIH2	0.586169984	0.0434393
TTC21B	0.58875977	0.00574126
MBIP	0.58899039	0.0185833
GTF3C6	0.589686471	0.0208099
TMEM123	0.590883247	0.00131613
HSPBAP1	0.592123493	0.0447555
CCNG1	0.592227341	0.00206129
TRIM44	0.594431305	0.000493027
SLC33A1	0.598622745	0.00274527
LASP1	0.599273714	0.00206129
CHKA	0.599612764	0.00459373
SYNJ2	0.600036015	0.0492685
SERPINI1	0.600148738	0.0424716
TXNL1	0.603000039	0.00430332
NEU1	0.603438646	0.00241048
ZRANB3	0.603989762	0.0290087
INPP1	0.604901859	0.0272819
ALCAM	0.606699068	0.00401827
WWC1	0.607977147	0.00401827
CAPN2	0.609368572	0.000923837
SLC39A7	0.610828381	0.00241048
APOF	0.611588846	0.0171412
MGAT4A	0.613089244	0.0267718
IFIT1	0.614262834	0.00659163
AKAP7	0.614623571	0.0157377
SNX6	0.617127291	0.00307913
TMEM106C	0.617893456	0.0480598
PRKAB1	0.617928577	0.0148244
RPS19BP1	0.618423051	0.0487735
RPP30	0.619780814	0.0431473
LY75	0.621461102	0.007639
FNDC3B	0.621630847	0.00401827
PIGX	0.622842372	0.0139214
AKIP1	0.623249619	0.0369299

siYap UP	Fold Change (siYap/siLuc)	q-value
FURIN	2.305260839	0.000493027
RERE	2.304350224	0.000493027
ARID1A	2.28337846	0.000493027
AKAP12	2.266694561	0.000493027
CPSF4L	2.2645588	0.0135152
FYCO1	2.255519877	0.000493027
SORL1	2.253410264	0.000493027
ASAP2	2.241819307	0.018368
MBNL3	2.241291039	0.00131613
TBX2	2.236697262	0.0274562
SLC17A3	2.236340707	0.000493027
ESAM	2.235519298	0.000493027
GATAD2B	2.231880834	0.000493027
SIK3	2.22391246	0.000493027
APOC4	2.212457895	0.000493027
GSTT1	2.211476635	0.000493027
IL18	2.207892606	0.000493027
TTYH3	2.20461999	0.00459373
DHRS1	2.202542718	0.000493027
AHDC1	2.188526723	0.00488988
TMEM104	2.184540723	0.0150704
ANXA11	2.171722848	0.000493027
HNF1A	2.168744351	0.000493027
FTH1	2.164119252	0.000493027
FOXA1	2.163834261	0.000493027
SPATA2L	2.160941475	0.0352232
NR0B2	2.157618804	0.00307913
CCDC57	2.156512383	0.00169137
CHD9	2.148172727	0.000493027
HDHD3	2.140725776	0.00868707
MTSS1L	2.13977633	0.0353808
TPCN1	2.13314199	0.000493027
ANKRD11	2.12652822	0.000493027
WNK4	2.111824578	0.0398945
AOX1	2.111297674	0.000493027
PPARG	2.105743919	0.000493027
VPS13D	2.092793551	0.000493027
SLC7A2	2.075069993	0.000923837
SEMA3F	2.072267146	0.00340081
SLC25A33	2.071247563	0.000493027
ETNK2	2.062479815	0.000493027
RELN	2.062022393	0.000493027
DNASE1L3	2.060593603	0.00574126
DDX19A	2.058594961	0.00241048
FABP1	2.055201716	0.000493027
TRIM25	2.055087755	0.000493027
TOM1	2.051927845	0.000923837
ZMIZ1	2.04786413	0.000923837
HSPG2	2.02763785	0.000493027
ERBB3	2.022836899	0.000493027
ABCC2	2.018788817	0.000493027
LARP1	2.001802995	0.000493027
DOCK4	1.994271733	0.000493027
ERRFI1	1.983847323	0.00241048
ACSS3	1.979613794	0.000493027
WIPF2	1.978539681	0.00603958
ETFA	1.976724755	0.000493027
SYNPO	1.975668643	0.00241048
TMEM170B	1.972762116	0.000493027
BCL2L1	1.966499746	0.000923837
ADH4	1.962622902	0.000493027
VAC14	1.959743717	0.00169137
ZHX2	1.95896144	0.00169137
NAV2	1.957191605	0.000493027
MAML3	1.955060157	0.0433059
ARHGEF2	1.953970925	0.00169137
ACSF3	1.953524027	0.00942814
PROX1	1.952320621	0.000493027
HSDL2	1.944261133	0.000493027
TET3	1.934564728	0.000493027
ASGR1	1.934431979	0.000493027
IRS1	1.933761672	0.000493027
HACL1	1.929684515	0.000493027
PRDX3	1.92747213	0.000493027
TOMM40L	1.923769566	0.0249324
RNF10	1.917346391	0.000493027
PAFAH2	1.911934368	0.000493027
MYO9A	1.910393721	0.000493027
CCDC90A	1.902790859	0.000493027
ACAT2	1.902090645	0.000923837
ATG4C	1.901011158	0.00169137
FSCN1	1.895194609	0.0329638
CEBPB	1.888594534	0.00241048
EPT1	1.884626977	0.000493027
ZNFX1	1.876580267	0.000493027
ACVR1	1.872691169	0.00371096
BCL6	1.864809165	0.00131613
HAS3	1.862181895	0.0314211
NR2F2	1.857470116	0.00131613
AGFG2	1.849571407	0.00241048
RNPEP	1.847677544	0.000493027
ATXN2L	1.843028014	0.00169137
ATF7IP	1.841895229	0.00307913
RFX7	1.840154627	0.00131613
NPC1	1.83400173	0.000493027
OPTN	1.833753857	0.000493027
SENP8	1.833333183	0.0448978
ARID5B	1.832553097	0.000493027
FAM107B	1.827004263	0.000493027
SSFA2	1.825117061	0.00169137
APOC3	1.822850191	0.000923837
GAN	1.816605307	0.0483301
SH3BGRL2	1.815980864	0.00131613
AP3M1	1.814330145	0.000493027
CARD10	1.813946618	0.0209776
AP1M1	1.809956469	0.00574126
ADI1	1.805360565	0.000493027
TGFBRAP1	1.801923796	0.00131613
UBAP2	1.801020996	0.018997
YARS	1.796120323	0.0310607
PRKAA2	1.79408594	0.000493027
PUM1	1.792352005	0.000923837
MADD	1.780874683	0.00738558
PER2	1.777132192	0.00371096
LYST	1.767714149	0.000493027
GTF2I	1.765005893	0.000493027
SEC24A	1.76428056	0.000493027
CCS	1.762357977	0.00131613
PON2	1.756453033	0.000493027

siYap DOWN	Fold Change (siYap/siLuc)	q-value
CCBL1	0.625511364	0.0155245
TMEM37	0.625852244	0.00868707
C8A	0.625893457	0.0267718
ENPP3	0.628389509	0.00274527
PTPN14	0.628487955	0.0290087
FAM129A	0.628699709	0.0295389
SAE1	0.629595005	0.0209776
MYL6	0.632794076	0.0101824
DCP2	0.634168885	0.007639
NDUFC2	0.635285061	0.00915859
ABCA9	0.637329789	0.0255536
TGIF1	0.637592251	0.0366459
GSTO1	0.637821662	0.0177869
SERTAD1	0.637935735	0.0448978
SLC44A3	0.638418339	0.00843096
CLIC1	0.639543325	0.0260823
FNBP1L	0.639925561	0.00631953
SDC2	0.643373313	0.0155245
PPP1R9A	0.645808798	0.0316105
DARS	0.645831628	0.0101824
NIF3L1	0.646902862	0.0282462
PRUNE	0.646989857	0.0269397
PRNP	0.647024389	0.0116801
ZBTB26	0.647999677	0.018368
TMEM141	0.649136597	0.0404303
LRRFIP1	0.653548406	0.0116801
GMFB	0.655289809	0.0137115
TRAM1	0.656908801	0.0196648
PTTG1IP	0.657347435	0.0114573
ABCC3	0.657487786	0.0290087
MYL12B	0.657965115	0.0135152
GTF2F1	0.658563747	0.0350541
REXO4	0.661599936	0.0219011
CRIPT	0.662453456	0.0293534
DNPEP	0.662743261	0.0260823
ING4	0.667531119	0.0291861
NEDD8	0.667780097	0.0293534
ANAPC5	0.67116668	0.0155245
STX7	0.67328396	0.0253528
ERMP1	0.674699501	0.0181714
CBX5	0.675052681	0.0267718
BIRC2	0.675443968	0.0247129
PGAP1	0.67750007	0.0293534
MPHOSPH10	0.679313768	0.0415232
TTC3	0.680174111	0.0387602
NME1	0.68125603	0.0333244
PSMD13	0.681472809	0.0243634
SRI	0.68195337	0.0253528
KPNA2	0.686267053	0.0280564
MTIF2	0.686277994	0.0269397
RPS11	0.687576909	0.0358941
SORBS1	0.688061774	0.0319978
TAP1	0.688182447	0.034029
DSE	0.68856464	0.0428537
CACYBP	0.690898172	0.0331496
IYD	0.691183652	0.037961
SPOPL	0.69220823	0.0444695
CEP170	0.695456893	0.0352232
CTNNA1	0.696097838	0.0483301
COX7A2L	0.696181316	0.0389186
PLIN3	0.696722471	0.037638
DHRS3	0.699486927	0.0410798
PKP2	0.700856506	0.0353808
MMD	0.701673606	0.0446127
UBXN4	0.702731269	0.0404303
PDCD10	0.709250418	0.0492685

siYap UP	Fold Change (siYap/siLuc)	q-value
PLXND1	1.754929409	0.000923837
MICALL1	1.744657689	0.0457327
COL4A3BP	1.744108751	0.000923837
PIGS	1.743684471	0.0333244
LRRC8D	1.734896984	0.00459373
PFKFB3	1.73235908	0.00371096
ZFP36L2	1.731911247	0.000493027
ZMYND8	1.729675017	0.00603958
TMEM184B	1.729509574	0.0205822
MYO1B	1.728587939	0.000493027
MRS2	1.720690949	0.00868707
FERMT2	1.717979713	0.000923837
SLC2A8	1.708702224	0.0463954
PM20D2	1.702336214	0.022703
PTK2B	1.697480498	0.00603958
PROZ	1.697393432	0.00241048
MTR	1.691023841	0.00816443
DGAT2	1.685678026	0.00307913
HPD	1.676783005	0.028417
XPA	1.674448495	0.00868707
ACOX1	1.672658586	0.0245595
CCNK	1.669926957	0.0257279
AGPAT6	1.6673246	0.00131613
DAB2IP	1.66727375	0.00686812
ELL2	1.66220463	0.00307913
DPP9	1.655884447	0.0146108
ZFYVE26	1.647588544	0.00603958
NFATC3	1.646564469	0.00430332
SLC31A1	1.633866377	0.00307913
LOXL2	1.632177546	0.00816443
CARD6	1.631486444	0.0185833
ITPR3	1.630820503	0.0179668
WASL	1.630715379	0.00241048
ANGPTL4	1.629693885	0.0116801
DSP	1.629141596	0.00518666
SNX33	1.623326277	0.0148244
RGL1	1.621954108	0.0118954
AGT	1.617993711	0.00993221
FKBP5	1.61647254	0.00603958
PTPN3	1.613745419	0.00915859
TMEM14C	1.606851939	0.00401827
ELL	1.603789724	0.0298699
PID1	1.603279553	0.00459373
CHD1L	1.59357288	0.0121176
GLT1D1	1.592782196	0.0209776
PSMD7	1.592172887	0.0257279
TNS1	1.588553854	0.00547498
HNRNPUL2	1.585929896	0.00488988
MTOR	1.585389141	0.00790866
RNF144B	1.585304527	0.0135152
CLIP1	1.58417092	0.00371096
KLF9	1.583659305	0.00738558
BAG6	1.581805263	0.0222807
MYLK	1.577889307	0.0130893
FAM193B	1.576378524	0.0362817
AFF1	1.57368632	0.0155245
PTCH1	1.573533616	0.0371047
STAU1	1.569623993	0.007639
ABCD3	1.568252649	0.0116801
IARS	1.568043954	0.007639
DCLRE1A	1.567738569	0.00968351
PLEC	1.564307354	0.012357
ARHGEF3	1.56253012	0.00790866
TLN1	1.5597448	0.0109721
USHBP1	1.559451841	0.0480598
PHLPP1	1.558687811	0.0181714
RBMS1	1.555608475	0.00843096
GPT2	1.555420868	0.0249324
FAT1	1.550399489	0.0121176
SEC31A	1.548595119	0.00915859
NCOA3	1.545534651	0.0133268
ALS2	1.544254998	0.018368
SMARCC2	1.538935749	0.0177869
NFKBIZ	1.533931438	0.0150704
WWC2	1.533698606	0.0360936
DQX1	1.528830007	0.0421366
TGFA	1.528654106	0.033704
PAOX	1.528589473	0.0239526
PDHA1	1.527743137	0.0220914
PTPRG	1.525449056	0.00915859
DNAJC25	1.522875498	0.0398945
CHD8	1.5213267	0.0171412
HIVEP2	1.516784367	0.0293534
CHN2	1.515514862	0.0249324
CDH2	1.512057497	0.0121176
PABPC4	1.509448986	0.0492685
CD44	1.509354825	0.0369299
YLPM1	1.509016938	0.0259012
NFE2L1	1.508585014	0.0213461
ATP2B1	1.506814686	0.0141726
KPNA6	1.505712157	0.0196648
SNTB1	1.501478691	0.0157377
GBP6	1.500395665	0.0217476
B4GALT1	1.498669227	0.0187908
SNX25	1.496699922	0.0333244
TGFBI	1.496024705	0.0247129
GSK3B	1.494816092	0.023371
HERPUD2	1.494356122	0.0278478
COASY	1.488917689	0.0213461
PPP1R15B	1.486703549	0.0211662
KLF3	1.476656229	0.0485053
FRMD4B	1.476504752	0.0255536
ARNT	1.471534126	0.0321959
CRIM1	1.471245497	0.0276568
TAPBP	1.470688798	0.0274562
DUSP6	1.465682889	0.0421366
PHACTR2	1.459391544	0.0455921
HOOK3	1.44476415	0.0358941
WNK1	1.441871903	0.0455921
ARID1B	1.438973476	0.0421366
FNIP1	1.434708854	0.0398945
ATP2A2	1.425792463	0.0479106
SLC17A2	1.425719332	0.0472442
BPHL	1.415284409	0.0428537

Table S2. Yap signature in advanced HCC (related to Figure 4).

Gene set defining a YAP-specific signature based on the integration of differentially expressed genes observed in siLuc-LNP-treated versus siYap-LNP-treated HCCs in DKO mice (day 9) with chromatin immunoprecipitation data for TEAD binding sites in hepatic cells (ENCODE database) (see also **Fig. S4E**). Genes are ranked based on fold-change expression.

Table S3

Gene name	*Forward primer (5' to 3')*	*Reverse primer (5' to 3')*
18S	TGCCTTCCTTGGATGTGGTAG	CGTCTGCCCTATCAACTTTCG
AKR1D1	TGGAGTGCCACCCGTATTTC	GGCTATGTGCGACAATGACG
B2M	GGTCTTTCTGGTGCTTGTCTCA	GTTCGGCTTCCCATTCTCC
BDH1	GGTGGAACCTGGCAACTTCAT	GGTCATCCCACATCTTCTTGG
CDC6	CTGAAGAGTGCAAAGCTCCG	GCTTGTGTCTGGGATCTGGT
CDK1	AAGTGTGGCCAGAAGTCGAG	TCGTCCAGGTTCTTGACGTG
CDT1	TTACCAGCTCACCATCGAGC	TCCTTGACACGTTCCACCAG
CIDEB	CAATGGCCTGCTAAGGTCAGT	GATCACAGACACGGAAGGGTC
CLML4	AAGCAGGCATTGAACCAAACG	AGGAATGGTGATCCTCTGGATAA
CTGF	AGCTGACCTGGAGGAAAACA	GACAGGCTTGGCGATTTTAG
DBF4	GACATTCGATACTACATTGAACAGA	TCTCCCTGTTCTTGTCTTTTGT
DHRS1	AAAAGCCTGTTCGAGCAAGTAG	CGCCAGCATAGGCATTATTGAC
DIO1	AGAGACTCGTAGATGACTTTGCC	GCCGGATGTCCACGTTGTT
E2F1	CAGCAACTGCAGGAGAGTGA	GTCCTGGCAGGTCACATAGG
ETFDH	TCTTCCGATGAACAATCATGGC	AGTGGCGATTCCTTTTACACTAC
HNF4a	GGTAGGGGAGAATGCGACTC	AAACTCCAGGGTGGTGTAGG
KI67	GCTCACCTGGTCACCATCAA	TGACACTACAGGCAGCTGGA
LGR5	CAGTGTTGTGCATTTGGGGG	CAAGGTCCCGCTCATCTTGA
MCM4	CAGGGGACAGAGTGAACGTC	ATGCAGACGTTTTGCATCCG
MCM6	CCTGAGAGAAACACGCTGGT	GGTCTTCAAGGCTCGACACA
MCM7	GCGCTTAAGGACTACGCGAT	CCGATGAGCCAGATGAACCA
MELK	GGCATCCTCCTGTATGTGCT	GCTACTGGGAGAGAGCCACT
NCPAG	GCCAAGTTTGTTACTTCATTTCACC	CTGCACTGCTGTTTGCTTCAT
NUF2	CGGCTGGAGCACTTCTACAT	CCGGCAAATGGGCATAAAGG
ORC1	TACGTGTTGTAGCCGTGGTC	GCCTTGGAGGTAGGATGGC
PBK	TGTTGGCGGGAGGGAG	TCCTTCCATTGTAGCAATCACG
POLA1	GACTGTAAACTGGAGGCAAGC	TCTCCCCAGCTTTAGCCTTTTT
RFC3	TGGCCCAGTCACAACAACTT	GTTCTGCGTAAGGCATGCTG
SOX9	GAGCCGGATCTGAAGAGGGA	GCTTGACGTGTGGCTTGTTC
TBX3	ATCACGAAGTCAGGAAGGCG	TATCGACAGTCGTCAGCAGC
UBE2T	TGGGGAAGGAGTCCCGTTTCTA	AGGTCTGGCGGGGGTGTA
YAP	GGATGTCTCAGGAATTGAGAACA	ATGCTGTAGCTGCTCATGCTGA

Table S3. Primer sets used in this study.

Set of primers used for expression analysis (qRT-PCR) for the indicated genes.

Supplemental Experimental Procedures

Materials

Reagents were obtained from the following sources: antibodies against YAP (Cell Signaling cat. #4912), SOX9 (Millipore cat. #AB5535), MST1 (Cell Signaling cat. #3682), Glutamine Synthetase (BD Transduction Laboratories cat. #610517), Ornithine aminotransferase (Abcam cat. #ab137679), β-Catenin (BD Transduction Laboratories cat. #610154), PCNA (Cell Signaling cat. #13110), Ki67 (Abcam cat. #ab15580), Cleaved Caspase-3 (Cell Signaling cat. #9661), GAPDH (Millipore cat. #AB374); biotinylated goat anti-rabbit (cat. #BA-1000) and anti-mouse (cat. #BA-9200) secondary antibodies from Vector Laboratories; RPMI, DMEM, DMEM:F12, Sodium Pyruvate (cat. #11360070), Insulin-Transferrin-Selenium-X (cat. #51500056), Insulin (cat. #12585014) and fetal bovine serum (FBS) from Life Technologies, Recombinant Human IGF-II (cat. #100-12) and EGF (cat. #AF-100-15) from PeproTech; Ad5CMV-Cre Adenovirus was purchased from the Gene Transfer Vector Core, University of Iowa (http://www.uiowa.edu/~gene/); Liquid Isofluorane for inhalation was purchased from Baxter (Forane, cat. # 1001936040).

siRNA-mediated *in vitro* knockdown

siRNA were transfected by using **Lipofectamine®** RNAiMAX Transfection Reagent (Life Technologies) at a final concentration of 20 nM. Control siRNA was purchased from Ambion (Negative Control #1 cat. #4390843) and anti-*Yap* siRNA was provided by Novartis (target sequence: 5'-TTAAGAAGTATCTTTGACC-3').

SDS-PAGE analysis

Cells or liver tissues were lysed in ice-cold RIPA lysis buffer (150 mM NaCl, 50 mM Tris-HCl (pH 8), 1mM EDTA, 1% NP-40, 0.5% Sodium Deoxycholate, 0.1% Sodium Dodecyl Sulfate) supplemented with one tablet of EDTA-free protease inhibitors [Roche] per 10 ml, Serine/threonine phosphatase inhibitor and Tyrosine Phosphatase inhibitor [Calbiochem]. Samples were sonicated and clarified by centrifugation and protein content measured using BCA protein assay kit (Thermo Scientific). 10µg protein was resolved on 10% SDS-PAGE gels and transferred onto PVDF membranes (GE Healthcare Life Sciences, Pittsburgh, PA). Membranes were blocked in Tris-buffered saline (TBS) containing 10% non-fat dry milk and 0.1% Tween 20 (TBS-T), prior to incubation with primary antibody overnight at 4°C. The membranes were then washed with TBS-T followed by exposure to the appropriate horseradish peroxidase-conjugated secondary antibody for 45 min and visualized on Kodak X-ray film using the enhanced chemiluminescence (ECL) detection system (Thermo Scientific).

Ultrasound imaging

Mice were anesthetized by inhalation of isoflurane at a starting dose of 4% with O2 1-2L/min and maintenance dose of 2% O2, and placed on a 40^0C heating platform in order to maintain their body temperature. Abdominal hair is shaved off using a Remington groomer. Aquasonic 100, an ultrasound transmission gel, was applied to the shaved abdomen and liver imaging was performed using a high frequency Broadband tranducer that allows the detection of lesions up to 0.5 mm. Images were captured using the associated Vevo software.

RNA Extraction from mouse HCC

6-10 mm^3 pieces of previously frozen liver tumors were homogenized in 700 µl of Trizol using scissors and syringe. 140 µl of Chloroform was added to the specimens before being vortexed for 30 seconds and incubated for 10 minutes at room temperature. The RNA-containing

aqueous upper phase was collected on ice after centrifugation (15min, 12,000g, 4°C) and mixed with ½ volume of High-salt solution (1.2 M NaCl; 0.8 M Sodium Citrate) and one volume of Isopropanol. Supernatant was removed after a 10min centrifugation (12,000g, 4°C) and the precipitated RNA was washed with ice-cold 80% ethanol. Washed RNA was spin down for 5min (7,500g, 4°C) and allowed to air-dry before resuspension in RNAse-free water.

Quantitative RT-PCR

Reverse transcription from total cellular RNA was performed from 2 µg of total RNA using the QuantiTect Reverse Transcription Kit (Qiagen). Quantitative RT-PCR was performed with FastStart Universal SYBR Green (Roche) in a MX3005P continuous fluorescence detector (Stratagene) or using a Lightcycler 480 (Roche). PCR reactions were performed in duplicate and the relative amount of cDNA was calculated by the comparative CT method using the 18S ribosomal RNA sequences or beta-2 microglobulin (B2M) as a control. Primer sequences can be found in **Table S3**.

Cell proliferation assay

Cells were plated in 6-well plates at 60,000-120,000 cells per well in 2 mL of complete culture media. At the indicated time points, cells were trypsinized and counted using a Countess automated cell counter (Invitrogen).

Cell Culture

DKO and TKO murine cell lines were generated from liver tumors that arose in *Mst1*$^{-}$*, Mst2*^{Flox}, and *Mst1*$^{-}$*, Mst2*^{Flox}*, Yap*^{Flox} mice, respectively, by performing collagenase/dispase-based cell isolation and maintained at low passage numbers. Cells were grown on collagen-I-coated plates and cultured in DMEM:F12 supplemented with 5% heat inactivated FBS, Sodium Pyruvate (1 mM), Insulin-Transferrin-Selenium-X, human EGF (50ng/ml), human IGF-II (30 ng/ml) and

Insulin (10 µg/ml). Negative mycoplasma contamination status of all cell lines and primary cells used in the study was established using LookOut Mycoplasma PCR Kit (Sigma, MP0035). Forced expression of *YAP* in TKO cells was performed by stable infection with a pBabe retroviral expression vector encoding human YAP.

Histology and immunostaining

Livers were harvested, submitted for histological examination, and analyzed in a blinded fashion by pathologist (V.D.). Tissue samples were fixed overnight in 4% buffered formaldehyde, and then embedded in paraffin and sectioned (5 µm thickness) by the DF/HCC Research Pathology Core. Haematoxylin and eosin staining was performed using standard methods. For immunohistochemistry, unstained slides were deparaffinized in xylenes (two treatments, 3 min each), rehydrated sequentially in ethanol (2 min in 100%, 2 min in 95%, 2 min in 80%,), and washed for 3 min in water. Slides were incubated for 20 min with 3% H_2O_2 at room temperature to block endogenous peroxidase activity and rinsed twice with water (3min each). Endogenous peroxidase activity was blocked by incubating deparaffinized tissue sections with 3% Hydrogen Peroxide (20 min; Fisher Scientific), and antigen retrieval was performed by boiling in 10 mM sodium citrate buffer (20 min, 95°C, pH 6). Sections were blocked 1 hour in TBS-0.05 % Tween 20 (Fisher Scientific)-10% Normal Goat Serum (Cell Signaling #5425), and incubated overnight at 4°C with primary antibody. Primary antibodies were diluted in blocking solution as follows: YAP (1:40), SOX9 (1:2000), Glutamine Synthtase (1:200), β-catenin (1:100), PCNA (1:10,000), Ki67 (1:100), Cleaved Caspase 3 (1:150), Ornithine aminotransferase (1:200). Specimens were then washed three times for 3 min each in PBST and incubated with biotinylated secondary antibodies (1:200, Vector Laboratories) in blocking solution for 45min at room temperature, followed by catalyzed signal amplification using the Vectastain Elite ABC kit (30 min; Vector Laboratories) Specimens were then washed three times in TBS-0.05 % Tween 20 and treated with ABC reagent (Vectastain ABC kit #PK-6100) for 30 min, followed by three washes for 3 min

each. Finally, slides were stained for peroxidase for 1-2 min with the DAB(di-aminebenzidine) substrate kit (SK-4100, Vector Laboratories), washed with water and counterstained with haematoxylin. Stained slides were photographed with an Olympus DP72 microscope. For quantification of Yap, Ki67 and PCNA staining in HCC following short term treatment with siYap-LNPs (Figure 4E,F and Figure S4A,B), % of positive HCC nuclei within individual tumor nodules were determined by IHC. One or two liver sections were stained per treated animal and every HCC nodule was analyzed.

Gene Expression Profiling

RNA-sequencing was performed using total RNA isolated from HCC's from mice following treatment with siYap-LNPs and siLuc-LNPs for 9 days. RNA quality was measured using an Agilent Bioanalyzer and RNA was quantified using Qubit Fluorometer (Life Technologies) before sequencing library generation. RNAseq libraries were prepared using the ScriptSeq Complete Gold Kit (Epicentre). RNAseq libraries were uniquely indexed with custom primers (SriptSeq) and run on MiSeq (Illumina) to confirm quality of the library before sequencing to deeper coverage using a HiSeq2500 (Illumina). Approximately 50 million reads per sample were obtained. Data was processed using a standard RNA-seq pipeline that used Trimmomatic to clip and trim the reads, used tophat2 to align the reads to mm10, and used cuffdiff to calculate differential expression.

Image analysis and Statistics

Image analysis was conducted using ImageJ software (NIH). To determine the percentage of GS positive hepatocytes (**Fig. 2C**), five to eight representative images of stained liver tissue per animal were acquired using a 4X objective lens on an Olympus DP72 microscope and processed in an 8-bit greyscale setting. All images were subjected to fixed thresholding to evaluate positively stained areas (in μm^2), and a ratio between summed positive areas and the

total surface area of the tissue section (in μm^2, excluding the venous regions) was calculated for each image. Percentage of GS positive hepatocytes represents the average ratio for a given genotype. Statistical analyses of results are expressed as mean ± SEM, unless otherwise specified. Significance was analyzed using 2-tailed Student's t test. A p value of less than 0.05 was considered statistically significant.

Liver function tests

Following a 28-day treatment with siRNA-LNP formulations, blood from wild type mice was collected by retro-orbital puncture and mixed with 3.8% sodium citrate buffer using a ratio of 1 part citrate: 9 parts blood. The plasma-containing upper phases were collected on ice after centrifugation (15min, 1,500g, 4°C), and conserved at -80°C until analysis. Blood chemistry analyses (AST, ALT and Tbili) on samples were performed by the Center for Comparative Medicine platform (Massachusetts General Hospital, Boston MA 02115).

Analysis of human HCC

Specimens from 111 HCC patients treated with surgical resection in 3 institutions belonging to the HCC Genomic Consortium: Mount Sinai School of Medicine in New York, Istituto Di Ricovero e Cura a Carattere Scientifico (IRCCS) Istituto Nazionale Tumori in Milan and Hospital Clinic in Barcelona. Gene expression data is published elsewhere (Chiang et al., 2008; Villanueva et al., 2011) (Villanueva et al Hepatology submitted). Presence of previously published signatures such as CTNNB1 mutation signature (Lachenmayer et al., 2012), NOTCH signature (Villanueva et al., 2012), Chiang 5 subclasses (Chiang et al., 2008) and Hoshida S1-S2-S3 classes (Hoshida et al., 2009) was determined using a nearest template prediction algorithm implemented in GenePattern as previously reported (Hoshida, 2010), based on a prediction confidence false discovery rate (FDR) cut-off of 0.05. Presence of YAP late activation signature was calculated using the same algorithm but a FDR of 0.25 was used as cut-off.

Presence of mutations in exon 3 of *CTNNB1* was analyzed by Sanger sequencing. Tissue sections were macrodissected to avoid contamination of non-cancerous liver tissue. Genomic DNA was isolated using the QIAamp® DNA FFPE tissue kit (Qiagen). One-hundred nanograms of DNA from both samples as well as positive and negative controls for CTNNB1 mutations were then amplified by PCR using two sets of primers that span the whole exon 3: P1-F CAATCTACTAATGCTAATACTGTTTCG and P1-R CCTCAGGATTGCCTTTACCA (1); P2-F GATTTGATGGAGTTGGACATGG and P2-R TGTTCTTGAGTGAAGGACTGAG(2). PCR was performed in a volume of 20µL reaction mixture containing 1.5mM MgCl2, 0.2mM of each dNTP, 0.125mM of each primer and 1U of Platinum Taq DNA Polymerase (Invitrogen). PCR products were then purified using ExoSAP-IT® and sequenced.